

FINE-GRAINED NON-CARBONATE PARTICLES EMBEDDED IN NERITIC TO PELAGIC LIMESTONES (LOCHKOVIAN TO EMSIAN, PRAGUE SYNFORM, CZECH REPUBLIC): COMPOSITION, PROVENANCE AND LINKS TO MAGNETIC SUSCEPTIBILITY AND GAMMA-RAY LOGS

Leona KOPTÍKOVÁ^{1,2}, Jindřich HLADIL¹, Ladislav SLAVÍK¹, Petr ČEJCHAN¹ & Ondřej BÁBEK^{3,4}

(11 figures, 4 tables, 2 plates)

¹*Institute of Geology AS CR, v.v.i., Rozvojová 269, 165 00 Prague 6, Czech Republic, e-mails: koptikova@gli.cas.cz, hladil@gli.cas.cz, slavik@gli.cas.cz, cejchan@gli.cas.cz*

²*Institute of Geology, Faculty of Science, Charles University in Prague, Albertov 6, 128 43 Prague 2, Czech Republic*

³*Department of Geological Sciences, Masaryk University, Kotlářská 2, 61137 Brno, Czech Republic*

⁴*Department of Geology, Palacký University, Tř. Svobody 26, 77146 Olomouc, Czech Republic*

ABSTRACT. Variations in non-carbonate impurities trapped in the Lower Devonian limestone stratal successions in the Prague Synform are studied, with particular emphasis on the composition and quantities of fine-mineral grain assemblages. Different assemblages are encountered for the Lochkovian, lower Emsian and Pragian. The Lochkovian (represented by the Lochkov Formation) is characterized by pyrite–pyrrhotite assemblages with lower abundance of iron oxides and oxyhydroxides (mostly goethite) whereas the Pragian (represented by the Praha Formation) shows relatively abundant iron oxides and oxyhydroxides (mostly hematite). Major changes in magnetic susceptibility and gamma-ray spectrometric logs also coincide with the Lochkovian/Pragian boundary. Maximum values of magnetic susceptibility and relatively high Th, K concentrations above the boundary correspond to the elevated amounts of barite and Ba concentrations. This level is interpreted as a significant interval with elevated delivery of impurities of aeolian origin, deceleration of sedimentation rate together with decreased carbonate productivity. REE distributions in the Lochkovian to lower Emsian are indicative of the aeolian origin of trapped impurities. Detrital zircons found in all three stages are considered to be also of aeolian origin.

KEYWORDS: non-carbonate impurities, limestones, magnetic susceptibility, gamma-ray spectrometry, REE distributions, atmospheric dust, Lower Devonian, Prague Synform.

1. Introduction

Qualitative and semiquantitative analysis of non-carbonate impurities as carriers of magnetic susceptibility (MS) and gamma-spectrometric (GRS) properties and whole-rock geochemical data allow us to discuss the possible provenance of these particulates as atmospheric dust delivered to the sedimentary environment. The MS stratigraphy method was primarily used for climatic studies in modern non-carbonate sediments such as loesses or lacustrine sediments (e.g. Heller & Evans, 1995; Allen et al., 1999) but is now applied also to the Mesozoic and Palaeozoic marine rocks (Crick et al., 1997a; 2000; 2001; Riquier et al., 2007; Ellwood et al., 2008; Da Silva et al., 2009; Hladil et al., 2009). For the first time Crick et al. (2001), Ellwood et al. (2000) and others postulated that MS logs in marine sediments are mostly generated from particles of paramagnetic and ferromagnetic properties whose concentrations vary due to eustatic, climatic and tectonic changes. Generally high MS values are connected with low sea levels where erosional activity is increased and land-derived weathering products can be supplied to the sea in higher amounts. In contrast, low values are

connected with high sea levels and reduced fluxes of detrital particles. Despite of this premise, inverse patterns of MS have been reported during the important Devonian transgressive events such as Kačák-*otomari* event, Lower Kellwasser Event, Lower *pumilio* or mid-*punctata* events (Crick et al., 1997b; 2002; Hladil & Pruner, 2001; Hladil, 2002; Hladil et al., 2006) where high MS values are connected with high sea level. During the last years, it also appeared that an important role is played by variations in the proportion of atmospheric dust delivered to the limestones (Hladil, 2002; Hladil et al., 2006, 2009 and this volume). Hladil et al. (2006) postulated that the elevated concentrations of complex impurities in the Eifelian–Frasnian platform limestones in Moravia are not directly related to lowstand sedimentary condensation levels but reflect elevated delivery of detrital and aeolian material on the platform. Dominant concentrations of smectite–illite, micas, goethite and subordinate pyrrhotite, pyrite, hematite, ilmenite, magnetite or pyroxenes were identified as the MS carriers. Koptíková et al. (2010) revealed first data on lithology, eustatic interpretations, MS, GRS of the Lower Devonian limestone in the Požár 3 Quarry and discussed the possible carriers of MS and

rock colour signal in the limestones using spectral reflectance (SR) tool on the background of MS, GRS and TOC data.

Outcrop GRS logging as a method developed originally for well logging in the 1960s (e.g. Lowder et al., 1964) is now used for detailed palaeoenvironmental studies and high-resolution stratigraphy in pure limestones (Aigner et al., 1995; Ruffell & Worden, 2000; Hladil, 2002; Raddadi et al., 2005; Hladil et al., 2000, 2006, 2009; Bábek et al., this volume). It provides us with a combination of geochemical data acquired by multielemental instrumental neutron activation analysis (INAA) and a detailed study of mineral phases in insoluble residues, is a very precise tool for the identification of environmental changes possibly related to the variation in “dusting” through time because concentrations of K and Th are considered to be related to the concentrations of siliciclastic particles in limestones (e.g., clay minerals, micas, feldspars etc.; see Rider, 1986; Fiet & Gorin, 2000; Bábek et al., 2007 and this volume; Machado et al., this volume).

The aim of this study is to compile and compare detailed mineralogical, geochemical and geophysical records of Lower Devonian limestone beds (Lochkovian to lower Emsian) in the in Požár 3 section (Prague Synform) using low-cost and effective high-resolution stratigraphic tools such as magnetic susceptibility (MS) and gamma-ray spectrometry logging (GRS). Such a complex and multidisciplinary data set on the Lower Devonian limestone beds has never been published yet. The only previous data on the Lower Devonian rocks from Morocco, NW Spain and Bolivian wells were

released by Ellwood et al. (2001), on Ordovician siliciclastics to Lower Devonian sandstones with carbonate cements and dolostones by Schneider et al. (2004) and on Lower Devonian sandstones from Luxemburg by Michel et al. (this volume).

2. Regional and geological setting

2.1. Location

The study area lies in the Teplá-Barrandian tectonic unit (Bohemicum terrane) in the central part of the Bohemian Massif in the central European Variscan Belt. A major part of the Bohemicum is formed by Late Neoproterozoic and Palaeozoic volcanosedimentary and sedimentary sequences (Cambrian to Middle Devonian). The Proterozoic unit was formed by the Cadomian Orogeny and separated from the overlying Palaeozoic unit by an unconformity. Both units were subsequently deformed by the Variscan Orogeny in the late Devonian and Carboniferous (Cháb et al., 2008; Melichar, 2004). The term Prague Synform, unlike the frequently used Prague Basin (sensu Havlíček, 1981; 1982), is preferred here to stress the tectonic evolution of this unit. The Prague Synform represents an erosional relict of unmetamorphosed Palaeozoic rocks within the Teplá-Barrandian Unit – a synform which was formed during the Late Devonian folding, thrusting and burial (Glasmacher et al., 2002; Melichar, 2004). The youngest rocks crop out in several belts in the inner part of the Prague Synform (Fig. 1), being characterized by carbonate sedimentation

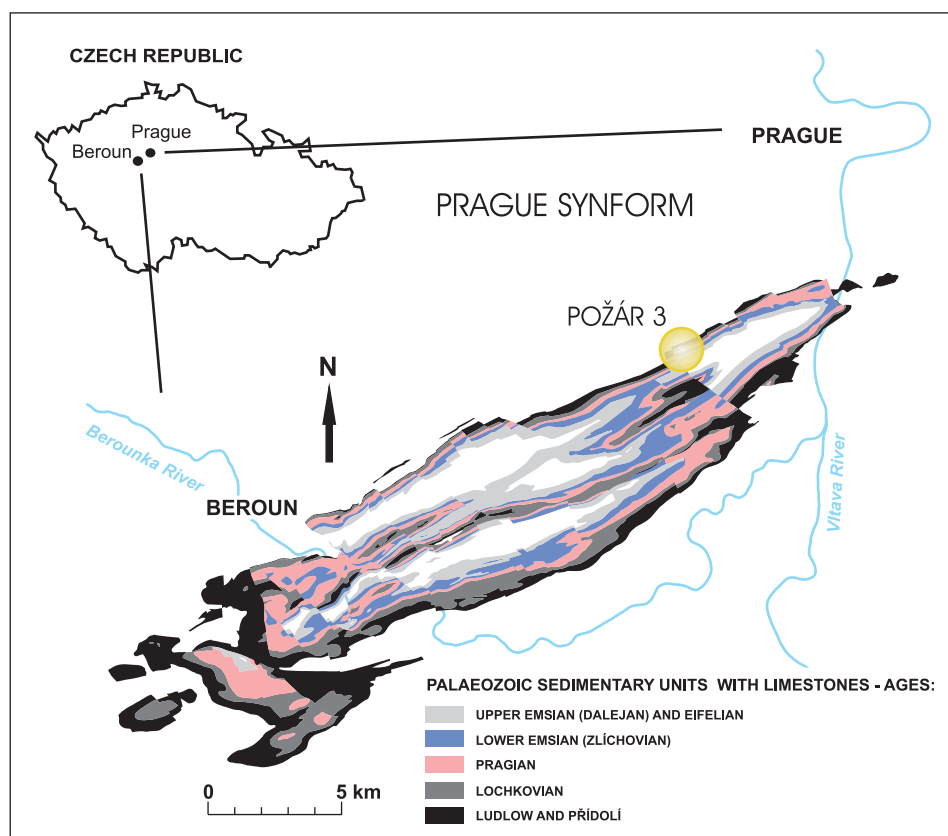


Figure 1. Location of the Prague Synform and position of studied section Požár 3 in a simplified geological map.

Chronostratigraphy of the carbonate sequences in the Prague Synform		Studied stratigraphic range
DEVONIAN	Middle	Givetian
		Eifelian
	Lower	Emsian
		Pragian
		Lochkovian
SILURIAN	Přídolí	
	Ludlow	

Figure 2. Stratigraphy of carbonate sequences in the Prague Synform with the studied interval outlined.

2004). A detailed biostratigraphic correlation may suggest a condensed sedimentation close to the Lochkovian/Pragian boundary (cf. conodont data by Slavík et al., 2007).

The Lochkov Formation has two lithotypes: the Radotín Limestone (0–23 m) and the Kotýs Limestone (23–77.6 m). The Radotín Limestone (redefined by Chlupáč, 1953) consists of cyclic or quasicyclic alternations of dark to medium grey sets of calciturbidites (calcisiltites to fine-grained skeletal grainstone, with normal grading, sharp bed surfaces in the middle part with scarce cherts) with weak shaly bands. Basal part differs from the rest of the lithotype in the presence of reddish and pinkish facies (mostly grainstones to rudstones dominated by crinoids). In the Kotýs Limestone lithotype (redefined by Chlupáč, 1953; 1981) calciturbidite material also prevails but consists mostly of fine-grained skeletal grainstones with lighter colours than in the underlying Radotín Limestone.

The overlying Praha Formation (77.65–118.1 m) is Pragian and mostly Emsian in age (Carls et al., 2008) according to the current GSSP of the Emsian base in the Kitab State Geological Reserve in Zinzilban range, Uzbekistan (Yolkin et al., 1997) and does not correspond to the original concept of duration and definition of the Pragian Stage in the stratotype area (Barrandian). Most of the Pragian in the original sense belongs to the Emsian, and the Pragian is approximately reduced to the interval of 77.6–91.2 m (see the correlation in Slavík et al., 2007). The Pragian age is characterized by the FOD of conodont taxon *Icriodus steinachensis* beta (81.25 m), but the “true” beginning of the Pragian can be estimated at a lower level (~76.0 m); precise delimitation of the local basal Pragian boundary is, however, constricted by scarcity of conodont time marks. The Praha Formation is the most diversified stratigraphic unit in the Prague Synform and is divided into five members (Chlupáč, 1981; Chlupáč et al., 1998): the Koněprusy Limestone, here called the “false” Koněprusy Limestone (77.6–80.25 m) because of slight differences from its definition as redefined by Chlupáč (1981), the Slivenec Limestone (80.25–85 m), Loděnice Limestone (85–104 m), Řeporyje Limestone (104–110 m) and Dvorce-Prokop Limestone (110–118.1 m). The thin blanket of the Koněprusy Limestone is represented by light grey to pinkish thick-bedded coarse, highly cemented bioclastic limestones dominated by altered crinoid fragments. The stratigraphically higher pinkish Slivenec Limestone is represented by thin-bedded amalgamated bioclastic limestone beds, mostly by crinoidal multimodal (up to tetramodal) limestones. Their grain-size distribution ranges from mud to sand and gravel. These are overlain by darker and variegated nodular calcisiltites with abundant dacroconarids of the Loděnice Limestone. Above, they pass into red nodular calcisiltitic Řeporyje Limestone with abundant dacroconarids. The Dvorce-Prokop Limestone, as the uppermost parts of the Praha Formation, consists of medium-grey thin-bedded calcisiltites and biomicrites with abundant ichnofabrics (*Zoophycos* isp.sensu Uchman, 1998 and *Chondrites* isp.

(Ludlow – late Eifelian/lowermost Givetian; Fig. 2). Carbonate production was replaced by siliciclastic input (black shale sedimentation) due to basin re-configuration in the Givetian as a consequence of the incipient Variscan Orogeny.

Section Požár 3 is situated in the W face of an active quarry on the western margin of Prague, 1 km ESE from the Řeporyje village. This section provides a unique uninterrupted 125 m-thick stratal succession of Lower Devonian sediments: limestone beds of Lochkovian to the lower part of the Emsian (Zlíchovian). GPS coordinates of the section are 50°01'39.35" and 14°19'38.74".

2.2. Stratigraphy

Biostratigraphy of the Požár 3 section is based on conodont stratigraphy and dacroconarids (Slavík, 2004a, b; Carls et al., 2007; Slavík et al., 2007) and comparisons with neighbouring sections (150 m E of Požár 3) – Požár 1 (with the Přídolí stratotype) – Požár 2 where detailed conodont biostratigraphy was established. The section Požár 3 belongs to three formations – the Lochkov Formation (0–77.6 m), Praha Formation (77.6–118.10 m) and Zlíchov Formation (118.1–125 m) – which are further subdivided into lithotypes whose definitions were outlined by Chlupáč et al. (1998). The age of the Lochkov Formation is Lochkovian to earliest Pragian. Detailed comparisons between the conodont successions and MS logs (Vacek, 2007) in both neighboring sections (Požár 3 and Požár 1) are indicative that, approximately 5 metres of strata are missing from the base of the Devonian in the Požár 3 section. The base of the Devonian in the Požár 1 section is determined by the entry of *Icriodus hesperius* Klapper & Murphy 1974 (Carls et al., 2007). The Pragian age of the uppermost part of the Lochkov Formation (~76.0 to 77.65 m) is likely. This can be expected due to comparison of faunal distribution with the Pragian stratotype at Velká Chuchle – Homolka (Slavík & Hladil,

sensu Fu, 1991). Slightly above the base of the Dvorce-Prokop Limestone, the so-called “Graptolite event interval” or “Graptolite horizon” (Hladil et al., 1996; Hladil & Kalvoda, 1997) occurs at 112.7–113.6 m. It is marked by a set of 8 dark shale graptolite-bearing turbidite beds with high amounts of glauconite and colonized hardgrounds. The presence of this interval is restricted to the NW flank of the Prague Synform and is characterized by the acme of dactyconarid *Guerichina strangulata* and conodont *Icriodus bilatericrescens gracilis* which enters closely below the interval in several Pragian/Zlíchovian sections (Slavík, 2004a). Following the correlation in Slavík et al. (2007) and Carls et al. (2008), this interval is close to the traditional Emsian base (Ulmen Gruppe) in Germany. Basal parts of the Zlíchov Formation (above 118.1 m) consist of the Zlíchov Limestone – thin-bedded calcisiltites, fine grainstones to dark-grey grainstones. This interval is marked by the disappearance of the dactyconarid *Nowakia* ex gr. *acuarina* just below the base of the Zlíchov Formation and FOD of *Nowakia zlichovensis*.

3. Methods

3.1 Lithological characteristics and facies analysis

Covered thin sections (in total 114 thin sections which represent each 0.5 to 2 m of the studied interval) were studied by optical microscopy, and data were processed

using a routine grain-size distribution analysis (Wentworth, 1922; Flügel, 2004). Acquired data represent semiquantitative sets of information on grain-size distributions of carbonate material along lines across each thin section. Categories significant ($\geq 20\%$), accessory ($\geq 5\%$) were used and quantities below 0.25% were omitted.

3.2. Mineralogical characteristics of insoluble residues and whole-rock geochemistry

Altogether 38 samples from the studied interval were analysed and investigated for insoluble residue mineral composition. Samples were selected to represent MS maxima, minima and medium values. We applied fast dissolution in concentrated hydrochloric acid. Light and heavy fraction assemblages were obtained by separation in heavy liquid (bromoform; density 2.83 g.cm^{-3}) using a Chirana centrifuge with 3000 rounds per minute. X-ray techniques (EDX JEOL JXA-50A and RTG Phillips X PERT PW3020) and SEM-EMP analyses (Cameca SX 100) were applied to identify mineral phases. Additional 4 samples (10–50 kg) were processed as fine-crushed whole-rock samples without acid dissolution and using gravitational, flotation, density and electromagnetic techniques (a Wilfley table, a Chirana centrifuge, a magnetic separator using current of 0.2 to 10 A, separation in acetylene tetrabromide and methylene iodide heavy liquids).

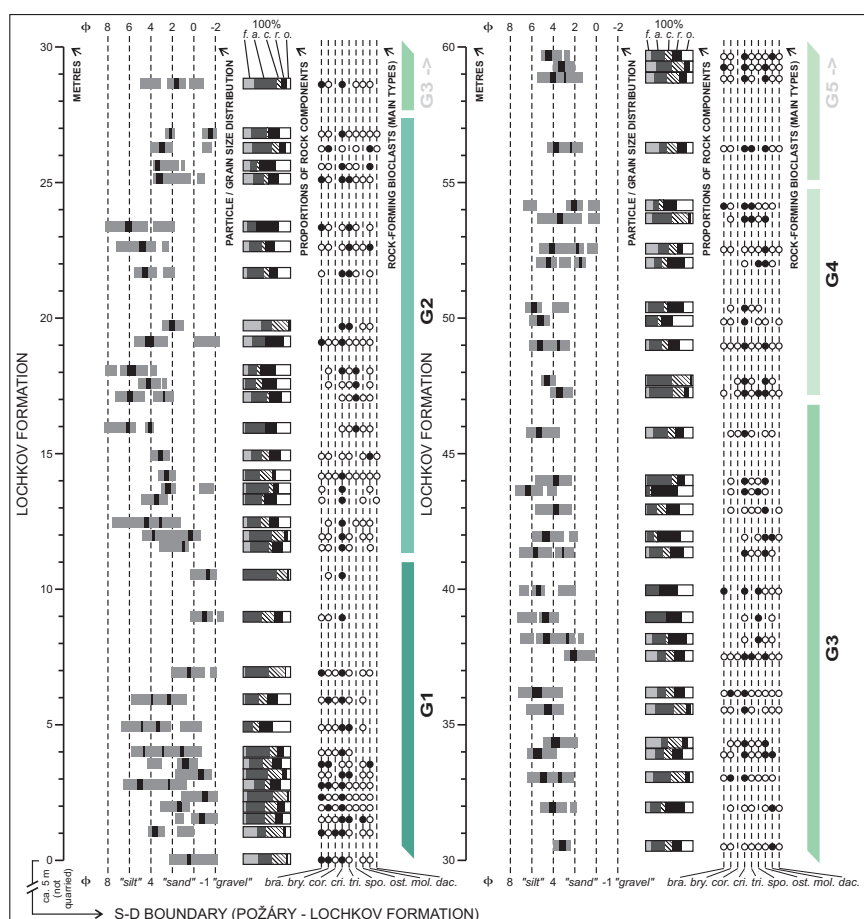


Figure 3. Lithological parameters from thin sections image analyses of the Lochkov Fm. and lower part of the Praha Fm. f. a. c. r. o.: f = fresh bioclasts, a = altered bioclasts and bioclastic rocks & cement fragments, c = cements and structures after the original cements, r = residues of dissolution sutures and microstylolitic bands, with accompanying populations of early diagenetic small carbonate rhombohedra, o = other, mostly unclear components, e.g. completely changed possible bioclastic, bioclastic/lithoclastic, bioerosional, and crystalloclastic-and-again-recrystallized fine particulate materials. bra. bry. cor. cri. tri. spo. ost. mol. dac.: bioclasts from bra. = brachiopods, bry. = bryozoans, cor. = solitary rugose and pachyporid tabulate corals, cri. = mostly crinoids, less other echinoderms, tri. = trilobites, spo. = sponge spicules, ost. = ostracod shells, mol. = molluscs (gastropods, cephalopods, bivalves, rostroconchs), dac. = dactyconarids (styliolinitids, nowakiids and various tentaculitoid shells). G1-G5 – GRS-MS segmentation, green and violet colours indicate differences in the concentrations of U (green colour) and Th (violet colour). For the detailed description of the segments see 4.2 and Fig. 5.

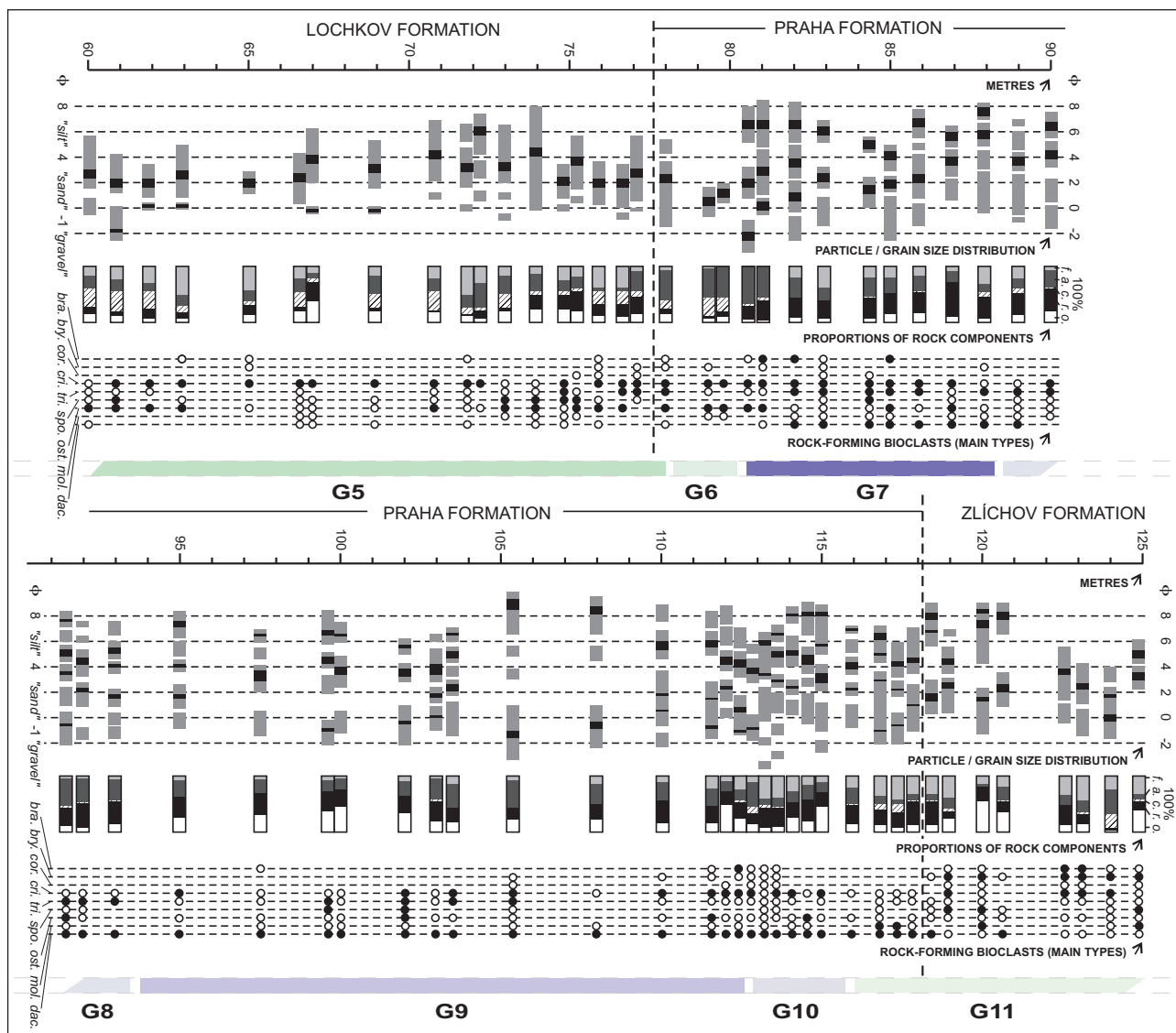


Figure 4. Lithological parameters from thin sections image analyses of the Praha Fm. and Zlíčov Fm. – a continuation from the Fig. 3. G5 – G11 – GRS-MS segmentation, green and violet colours indicate differences in the concentrations of U (green colour) and Th (violet colour). For the detailed description see 4.2, Fig. 5 and Table 2.

Forty-element instrumental neutron activation analysis (INAA) was applied to obtain whole-rock geochemical data sets, and realized at the Institute of Nuclear Physics AS CR, v.v.i. at Řez near Prague. Detailed methodology and technical aspects are reported in Řanda & Kreisinger (1983) or Řanda et al. (2007). Numbers of samples and sampling points were identical as for insoluble residues. The results were based mostly on Post-Archaean Australian Shale (PAAS) and Lu-normalized data of rare earth element (REE) group.

3.3. CaCO_3 content

Concentrations of CaCO_3 and total organic carbon (TOC) were analyzed in the Laboratory of Organic Geochemistry (Geological Institute, Slovak Academy of Sciences) in Banská Bystrica using C - MAT 5500 (Ströhlein). Homogenized and dried (at 110 °C) samples (two sets of 0.05 g, one of them was dissolved in hydrochloric acid) were combusted in a stream of pure oxygen at 50 °C to

1 000 °C, and CO_2 concentrations were analyzed in infrared carbon analyzers. CaCO_3 content was calculated as a difference between the two sets of samples. In total, 35 samples were analyzed and the error for each measurement was $\pm 4\%$.

3.4. Field gamma-ray spectrometry (GRS)

Field gamma-ray spectrometric measurements using a GR-320 enviSPEC portable gamma spectrometer (Exploranium, Canada; with NaI (Tl) $3 \times 3''$ detector and readings in selected 120 s period) were taken in the studied interval 123.6 m thick. Step of sampling was 0.5 m for the Lochkov Fm. (0–77.5 m) and 0.25 m for the Praha and Zlíčov Fms (77.6–123.6 m) with the probe held perpendicular to the rock wall at each sampling point. The contents of radionuclides ^{40}K (expressed in %), ^{238}U , ^{232}Th (expressed in ppm) and total natural gamma-ray (tot eU expressed in ppm) were determined. The error of measurement was calculated at $\pm 7.5\%$ for each element. In total, 338 measurements were taken.

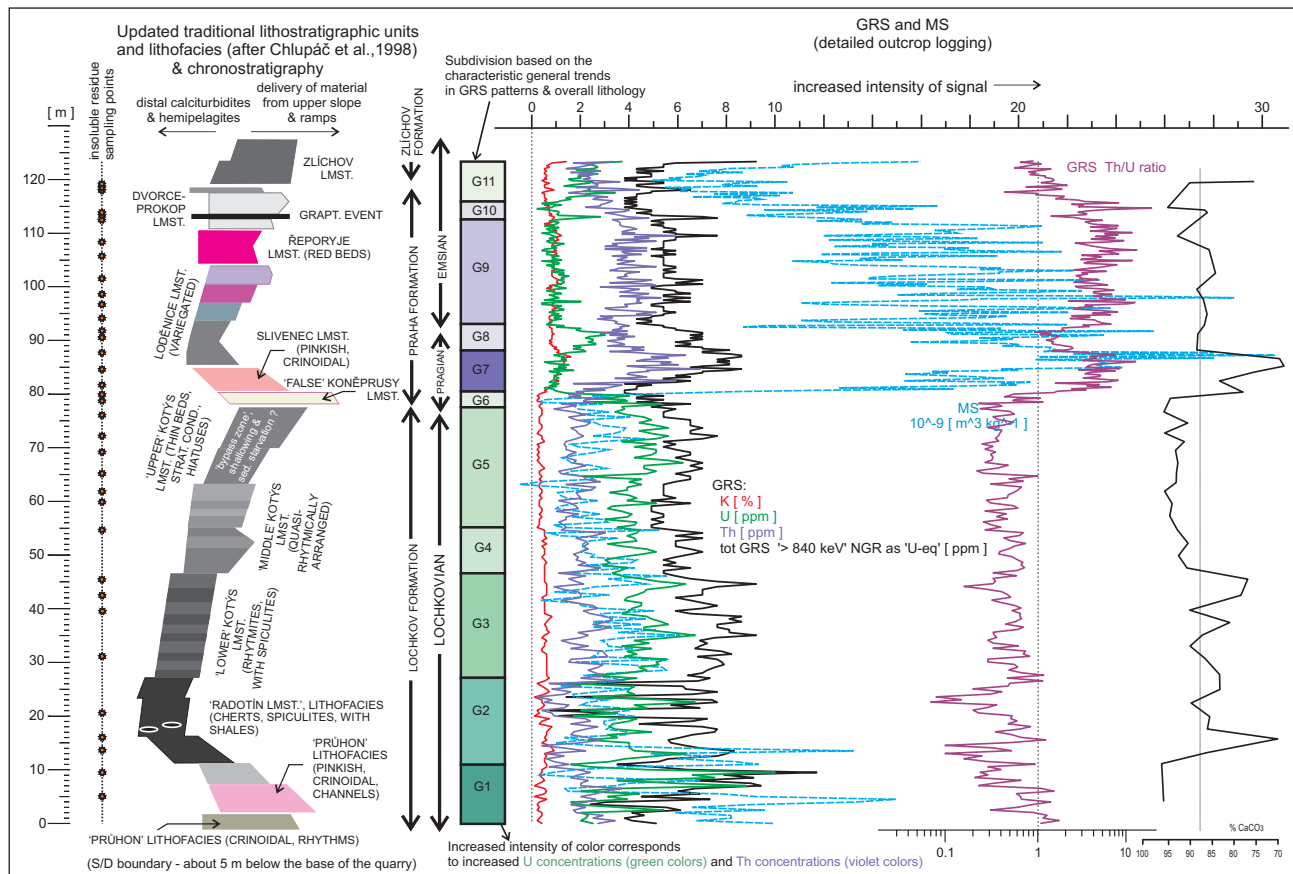


Figure 5. Overall MS and GRS logs together with lithological characteristics (based on the traditional lithostratigraphic members and biostratigraphy, see Chlupáč et al., 1998; here refined and modified – Kotýs Limestone) are plotted against the lithological subdivision based on the characteristic packages of GRS-MS patterns. Green and violet colours highlight variations in the U and Th concentrations. For their mean values and statistical characteristics see Table 2. Left column with orange stars – insoluble residue sampling points.

3.5. Laboratory magnetic susceptibility (MS) measurements

MS measurements of fresh rock samples were carried out in the Laboratory of Geological Processes of the Institute of Geology AS CR, v.v.i. in Prague using the KLY-2 Kappabridge (Agico Brno, Czech Republic; magnetic field intensity of $300 \text{ A}\cdot\text{m}^{-1}$, operating frequency of 920 Hz, sensitivity of $4 \cdot 10^{-8} \text{ SI}$) with the error of measurement of $\pm 2 \%$. Raw and normalized data on mass-specific MS, expressed in $\text{m}^3/\text{kg} \times 10^{-9}$, were plotted. Sampling rows were spaced each 10 centimetres in the Lochkov and Zlíchov formations and 5 centimetres in the Praha Formation (average 20–45 g per sample). Total thickness of the measured interval is 123.6 m (in total 1693 samples and measurements).

4. Results

4.1. Facies analysis and lithological characteristics

Detailed characteristics of lithotype components, their grain-size distributions, proportions of fresh bioclasts, altered material, residues of cement and dissolution seams are shown in Figs 3 and 4. Variations in the CaCO_3 content through the studied interval are figured in Fig. 5. A detailed study of lithology at section Požár 3 allowed us to make a finer subdivision of the traditional concept of

members as understood by Chlupáč et al. (1998) according to the GRS-MS characteristics (see 4.2.; Fig. 5; Table 1).

The Radoťín (11–23 m) and Kotýs Limestone (23–77.5 m) lithotypes of the Lochkov Fm. are thin-bedded, dark to medium-grey calcisiltites and fine-grained grainstones with thin shale intercalations and scarce cherts. They involve symmetrical cycles consisting of alternations of these black shales representing background sedimentation and calciturbidites which point to the depositional environment on the lower and middle parts of the slope. The ratio of fresh vs. altered skeletal fragments is the same as the ratio of cements vs. dissolution seams. Grain-size distributions are unimodal to slightly bimodal. Crinoid fragments dominate, ostracods, sponge spicules, trilobites are abundant and bryozoa, brachiopod shells and coral fragments also occur. The Radoťín Limestone is characterized by the presence of cherts and spiculites (Plate 2 – B) (although spiculites occur also in the Kotýs Limestone) and by elevated GRS-U concentrations and fluctuating K concentrations. Basal part of the Lochkov Fm. markedly differs from the Radoťín Limestone in its colour – it is pinkish to red and consists mostly of sparry crinoidal calcarenites–calcirudites (see Plate 2 – A). It was called the Průhon lithofacies after the traditional geographical name of the site where quarries Požár 1 to Požár 3 were later founded. The sediments display

elevated MS values and GRS-U concentrations. Their depositional environment seems to be relatively shallower (upper to middle parts of the slope) than that of the overlying Radotín Limestone, as suggested by wavy lamination (around 4.5 m), a higher proportion of shallow-water allochems and their multimodality. They may therefore represent channellized upper parts of the slope. The Kotýs Limestone was divided into three parts (Lower 23–46.5 m, Middle 46.5–55 m and Upper 63–77.5 m) also based on its GRS-MS characteristics, rhythm arrangement and colour. Fine-grained skeletal grainstones gain prevalence from the Lower to the Upper Kotýs Limestone and hemipelagic component is less abundant. The Lower Kotýs Limestone is characterized by slightly higher total GRS values (generally by higher U contents) and stable K concentrations than the rest of the Kotýs Limestone. The Middle Kotýs Limestone is separated into two GRS-MS segments (G4 and G5) based on the variation in K and Th concentrations. The Upper Kotýs Limestone is marked by slower rates of sedimentation as suggested by higher abundance of tentaculitoids and sponge spicules (Plate 2 – C), information from conodont data shows possible condensation around the Lochkovian-Pragian boundary (cf. data by Slavík et al., 2007). The overlying unit of the “false” Koněprusy Limestone (77.5–80.25 m; Plate 2 – D) consists of whitish and light grey crinoidal calcarenites–calcirudites which are almost strictly unimodal. They are dominated by altered crinoidal fragments delivered from the upper slope and ramps. The proportion of calcite

reaches its maximum. Stratigraphically higher, the number of modes in the grain-size distribution curve significantly increases up to four (Slivenec Limestone 80.25–85; Plate 2 – E), which is associated with the maximum regression level at the base of the Pragian. This so-called Lochkovian-Pragian boundary Event (Chlupáč & Kukal, 1988; Walliser 1996) is also well documented not only from Europe including Carnic Alps, Sardinia, Armorican Massif (Chlupáč & Kukal, 1988 and citations ibidem), but also from central Asia (Koren et al., 2007) or western North America (Johnson & Murphy, 1984 or Johnson et al., 1985).

The Slivenec Limestone shows typical calciturbidite characteristics: imbricated bioclasts (mostly large pluricolumnals of crinoids), truncated bases and amalgamated beds. Stromatactis-type cavities (filled with sparry calcite, some aborted or filled with greenish to yellowish dolomitic matrix with dispersed pyrite; Fig. 6 – C) are also present. This greenish to yellowish matrix fills inner spaces of large nautiloids (Fig. 6 – A, B). Fresh skeletal material is less abundant and the proportion of cement is reduced (Slivenec to Slivenec/Loděnice Limestone transition). This reduction was caused by multimodal grain-size distribution, pressure solution and compaction, so limestone beds have undulated surfaces. Pinkish, upward-thinning micritic crinoidal calcarenites belong to the darker and variegated Loděnice Limestone (85–104 m; Plate 2 – F) where tentaculitoids prevail together with trilobites and crinoids. They are overlain by

GRS-MS segment	base of the segment [m]	upper end of the segment [m]	thickness [m]	Granularity – (Φ) approx., mean	Granularity – (Φ) approx., range	polymodality	% of cements	% of diagenetic dissolution residues	pelagic/benthic – skeletal mass	dominant skeletal components	predominant rock types
G1	0	11	11	2	9	2	28	14	0.03	crin.	grainstones/rudstones
G2	11	27	16	4	10	2	16	27	0.14	crin. – sponge – tril.	carbonated mudstones/packstones
G3	27	47	20	5	7	2	21	31	0.45	crin. – sponge – ostr.	carbonated-mud supported, fine grainstones
G4	46.5	55	8.5	3	7	2	23	23	0.41	crin. – ostr. – tril.	carbonated-mud supported, grainstones
G5	55	78	23	3	8	2	25	16	0.38	crin. – ostr. – tril.	carbonated-mud supported, grainstones
G6	77.5	80.25	2.75	1	9	1	27	8	0.08	crin. – ostr.	grainstones/rudstones
G7	80.25	88	7.75	3	11	3	3	30	0.45	crin. – dacryo – tril.	grainstones to fine grainstones, calcisiltites
G8	88	93	5	3	12	5	2	33	0.78	dacryo	calcisiltites
G9	93	112.7	19.3	2	12	4	1	29	0.95	dacryo	calcisiltites and carbonated muds
G10	112.7	116	3.3	3	11	5	5	26	0.68	dacryo	calcisiltites and grainstones
G11	116	125	9	2	9	3	11	22	0.47	dacryo	calcisiltites and grainstones

Table 1. General lithological characteristics of GRS-MS segments. Abbreviations of skeletal components: crin. – crinoids, sponge – sponge spicules, tril. – trilobites, ostr. – ostracods, dacryo – dacryoconarids.



Figure 6. Large nautiloid shells from the Slivenec Limestone (A, B), and aborted stromatactis (C) filled with greenish to yellowish dolomitic matrix with dispersed pyrite.

pelagic redbeds (mostly with dactyloconarids and bored bioclasts) of the Řeporyje Limestone (Plate 2 – G) which represent maximum condensation, reflecting slower rate of sedimentation in the pelagic to slope to toe-of-the-slope sediments. Higher up, they are replaced by dark grey dactyloconarid Dvorce-Prokop Limestone (104–118 m), calcisiltites alternating with carbonate pelagic muds with abundant ichnofabrics (*Chondrites* isp. and *Zoophycos* isp.). A graptolite event (a set of 8 calciturbidite beds with flat surfaces; Plate 2 – H – fifth bed) close to the base of this unit represents a background sedimentation. Limestone beds of the Zlíčov Fm. (118–123.5 m) have a higher thickness, frequency and a darker colour: they are characterized by sparry calcarenites alternating with background sediment (black shale intercalations; Plate 2 – I).

4.2. MS, GRS and CaCO₃ content

Variations in GRS and MS logs permitted to divide the entire section into 11 GRS-MS segments (G1-G11; Fig. 5), based on characteristic patterns and variations in the concentrations of K, U and particularly Th (see Table 2). Both GRS and MS logs reveal major changes close to the Lochkovian/Pragian boundary. The MS log is characterized by four to five times higher values with high-amplitude oscillations in the Praha Fm. (mean $15.7 \text{ m}^3/\text{kg} \times 10^{-9}$) than in the Lochkov Fm. (mean $3.6 \text{ m}^3/\text{kg} \times 10^{-9}$). The GRS log shows a point of reversal in the Th/U ratio. Generally, the GRS log in the whole Lochkov Fm. is driven by dominant concentrations of U (mean 4.20 ppm and Th/U ratio 0.5). The opposite is true for the Praha Fm. where Th concentrations dominate (mean 3.7 ppm and Th/U ratio 3.9). The Zlíčov Fm. is characterized by a

slight dominance of Th (mean 2.49 and Th/U ratio 1.15). K concentrations are also higher in the Praha Fm. (mean 0.8%) than in the Lochkov Fm. (0.45 %) and Zlíčov Fm. (0.63 %). Approximate amounts of non-carbonate impurities were calculated both from the GRS data and INAA analyses (bracketed). Values are 6.81 (3.9) wt.% for the Lochkov Fm. and 9.94 (7.09) wt.% for the Zlíčov Fm. The highest values were recorded in the Praha Fm.: 13 (8.53) wt.%.

Limestones of the Lochkov Fm. has average CaCO₃ content 88 wt.% (89 wt.% for the Radotín Limestone, 80 wt.% for the Lower Kotýs Limestone, 90 wt.% for the Middle Kotýs Limestone, 94 wt.% for the Upper Kotýs Limestone). Limestones of the Praha Fm. has average CaCO₃ content 86 wt.% (96 wt.% for the “false” Koněprusy Limestone, 79 wt.% for the Slivenec Limestone, 83 wt.% for the Loděnice Limestone, 85 wt.% for the Řeporyje Limestone and 91 wt.% for the Dvorce-Prokop Limestone), Zlíčov Limestone of the Zlíčov Fm. has average CaCO₃ content 83 wt.%.

Generally, the Lochkov and Zlíčov formations show typical patterns of low-MS and high-U (with low Th concentrations) calciturbidites and low-carbonate background sedimentation. In contrast, the Praha Fm. shows generally high MS, Th and K patterns. As it is showed in Fig. 5 and in Koptíková et al. (2010), K and Th concentrations correlate through the section and the maxima in their concentrations correspond to the levels of minima of the CaCO₃ content. Variations in the K, Th, CaCO₃ concentrations and MS are interpreted in terms of regressive-transgressive cyclicity (Koptíková et al., 2010). In the lower parts of the Lochkov Fm., there is a transgressive trend (with landward shift of the facies with increasing concentrations of K and Th). Toward the

	No. of GRS measurements/ MS samples	Max value	Min value	Mean	Median	Standard deviation
G1	22/111					
MS		21.50	-0.59	6.06	4.75	5.42
K		0.60	0.10	0.36	0.40	0.15
U		10.00	1.60	4.07	3.45	2.38
Th		3.70	0.60	2.26	2.20	0.66
Th/U		1.70	0.70	0.75	0.65	0.45
G2	32/160					
MS		21.46	-1.55	3.92	3.19	3.31
		0.90	0.10	0.50	0.50	0.20
U		6.70	1.40	3.74	3.95	1.22
Th		3.60	0.20	1.46	1.40	0.82
Th/U		1.75	0.11	0.44	0.38	0.31
G3	39/195					
MS		13.41	-1.07	3.34	3.17	2.58
K		0.80	0.40	0.56	0.60	0.09
U		6.70	2.50	4.63	4.60	0.81
Th		3.30	0.90	2.22	2.20	0.63
Th/U		1.16	0.16	0.50	0.49	0.19
G4	17/85					
MS		10.05	-0.63	2.60	2.43	2.07
K		0.60	0.40	0.50	0.50	0.06
U		5.10	2.90	3.86	3.90	0.64
Th		3.00	1.10	2.06	2.10	0.49
Th/U		0.74	0.27	0.54	0.57	0.14
G5	45/225					
MS		10.23	-1.42	2.17	1.99	1.64
K		0.50	0.20	0.33	0.30	0.08
U		6.20	2.10	4.34	4.30	0.80
Th		2.80	0.90	1.71	1.70	0.43
Th/U		1.00	0.22	0.41	0.37	0.15
G6	10/50					
MS		7.41	-0.50	1.74	1.65	1.60
K		0.40	0.20	0.29	0.30	0.07
U		5.30	2.20	3.65	3.75	0.96
Th		2.90	1.20	1.92	1.90	0.52
Th/U		1.14	0.23	0.58	0.52	0.29
G7	31/155					
MS		71.53	3.95	18.93	19.23	7.33
K		1.60	0.40	1.03	1.10	0.29
U		1.70	0.50	1.05	1.10	0.30
Th		6.90	1.70	4.28	4.30	1.30
Th/U		11.40	1.50	4.47	3.83	2.17
G8	20/100					
MS		51.30	6.68	19.26	18.72	6.78
K		1.10	0.70	0.83	0.80	0.12
U		3.00	1.00	2.19	2.20	0.52
Th		4.60	2.80	3.68	3.70	0.49
Th/U		3.60	0.93	1.82	1.67	0.65
G9	78/394					
MS		75.62	3.58	16.83	15.05	8.10
K		1.20	0.50	0.88	0.90	0.12
U		2.00	0.40	0.92	0.90	0.30
Th		5.90	2.70	3.95	3.85	0.65
Th/U		11.75	2.15	4.88	4.29	2.20
G10	14/66					
MS		30.63	6.09	11.44	9.97	4.70
K		0.90	0.50	0.71	0.70	0.11
U		2.80	0.20	1.09	1.05	0.63
Th		4.80	2.20	3.37	3.35	0.64
Th/U		17.00	1.39	4.38	3.16	3.93
G11	30/152					
MS		32.13	3.35	8.35	6.84	4.41
K		1.40	0.40	0.60	0.50	0.19
U		3.70	1.20	2.19	2.30	0.58
Th		4.40	1.40	2.48	2.45	0.67
Th/U		2.75	0.44	1.23	1.09	0.51

(K in %, U, Th in ppm; MS in $\text{m}^3 \cdot \text{kg}^{-1} \times 10^{-9}$)

Table 2. Average GRS and MS values and statistical characteristics of GRS-MS segments (for description see 4.2. and Fig. 5).

Lochkovian/Pragian boundary at the height around 80 m the CaCO_3 content increase and concentrations of K, Th decrease which is interpreted as a regressive trend with the basinward facies shift (Lochkovian-Pragian boundary Event level). Above this level the concentrations of K, Th, Th/U ration, MS values rapidly increase and CaCO_3 content decrease. Landward facies shift together with the reported aggradation of the Koněprusy reef complex in the Koněprusy area near Beroun (Chlupáč et al., 1998) suggest the transgressive pulse. Then concentrations of K, Th and MS values gradually decrease toward the Pragian/Emsian boundary (around 112–113 m) indicating regression up to the onset of the Zlíchov Fm.

4.2.1. MS and the red colour of limestones

Hematite in the red limestone from the Požár 3 section was identified using thermometric measurements and characteristic Curie temperature of 675 °C (Schnabl et al., 2009).

The interval with red colour of the limestones in the Praha Fm. (between 92.5 m and 112.5 m – upper part of the Loděnice Limestone and the Řeporyje Limestone) shows sharp boundaries and no facies changes on the borders. Spectral reflectance in visible light which is used routinely used as a proxy of TOC and CaCO_3 content and can be used also as a method how to estimate the concentration of chromophores such as hematite, goethite or chlorite was applied to the Požár 3 limestones (Koptíková et al., 2010). It has revealed that the colour carriers are diagenetic hematite and goethite, there is no correlation between red colour of limestones and MS, TOC and CaCO_3 content respectively. Colour boundaries well correspond to the changes in the Th/U ratio (increased values), well oxygenated bottom conditions and redox gradient at the bottom sediment which enable to precipitate hematite.

4.3. Mineralogy of non-carbonate particles

Mineral assemblages of heavy and light fractions of insoluble residues were studied separately using several

methods and steps. Light fraction of all studied samples is represented by ultra-fine porous structures that consists of crystalline to subcrystalline mixtures (Fig. 7 – A, B), and individual components are often smaller than 2 μm . This matrix is responsible for the bulk chemical composition and appearance of all insoluble residues. Polished surfaces of these aggregates revealed that grains of larger detrital or authigenic particles (euhedral or corroded grains) are very often enclosed in this material (Fig. 7 – C). These enclosings complicated the separation of light fraction from the heavy fraction: the accidental presence of a grain heavier than 2.83 $\text{g}\cdot\text{cm}^{-3}$ in all these aggregates (usually composed of fine grains lighter than 2.83 $\text{g}\cdot\text{cm}^{-3}$) shifted them to the heavy fraction. A rutile grain embedded in the aggregate of matrix is figured in Fig. 7 – D as an example. Light fraction assemblages yielded abundant quartz (Fig. 8 – A), dolomite, feldspars (orthoclase, microcline, albite – Fig. 8 – B, and plagioclase), clay minerals (Fig. 8 – C; kaolinite, montmorillonite) and muscovite. Together with barite (Fig. 8 – F), apatite (Fig. 8 – E), titanite, zircon (Fig. 8 – P, Q, R), rutile (Fig. 8 – O) and corundum from heavy mineral assemblages, they represent grains of diamagnetic properties with no influence on MS logging. All identified minerals and the locations of sampling points within the GRS-MS segments are listed in Table 3.

Particles of paramagnetic properties prevail in all three formations (Lochkov to Zlíchov Fm.) – grains of pyroxene and amphibole composition (Fig. 8 – J, K, L), olivine (Fig. 8 – N), epidote, pyrite (Fig. 8 – H, I), chalcocopyrite, chlorite (Fig. 8 – L), glauconite, dolomite rich in Fe, ankerite and clay minerals were identified. Grains of ferromagnetic properties include iron oxides (Fig. 8 – D; mostly hematite, often with high Ti content – up to several %, or goethite), ilmenite (Fig. 8 – M) and pyrrhotite (Fig. 8 – G) also contribute to the resulting MS log.

Another feature unusual for pure limestone is the occurrence of detrital zircons (Fig. 8 – P, Q, R). Zircons were identified at six stratigraphic levels in the Lochkov and Praha formations (in the GRS-MS segments G4, G5,

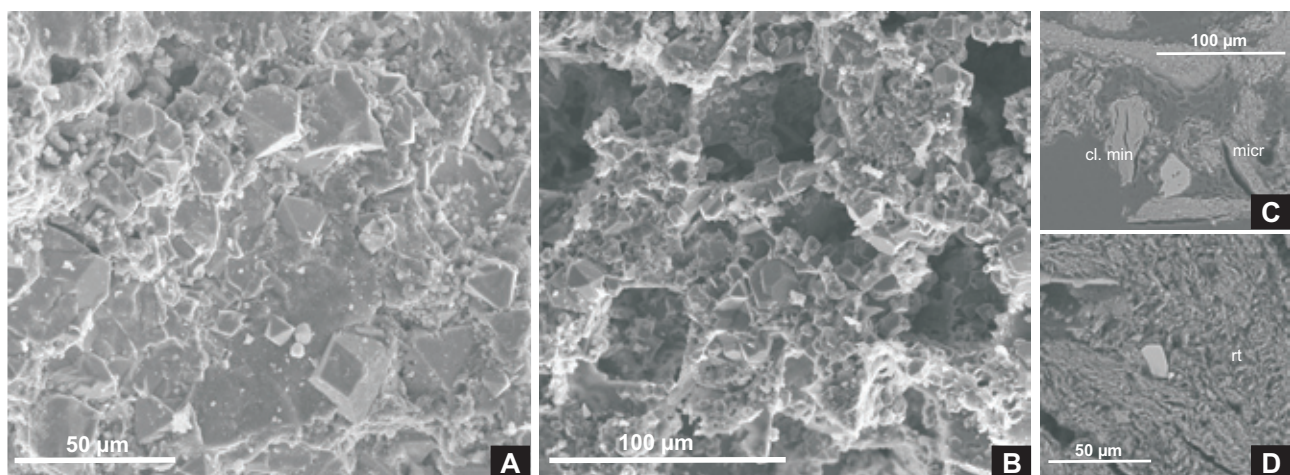


Figure 7. SEM images of typical appearance of light fraction aggregates (A, B; Lochkov Fm., 16.2 m). Detrital grains are often embedded in these aggregates of fine to subcrystalline porous matrix (Lochkov Fm., 9.7 m): C – grain of microcline (micr), D – grain of undistinguished clay mineral (cl min).

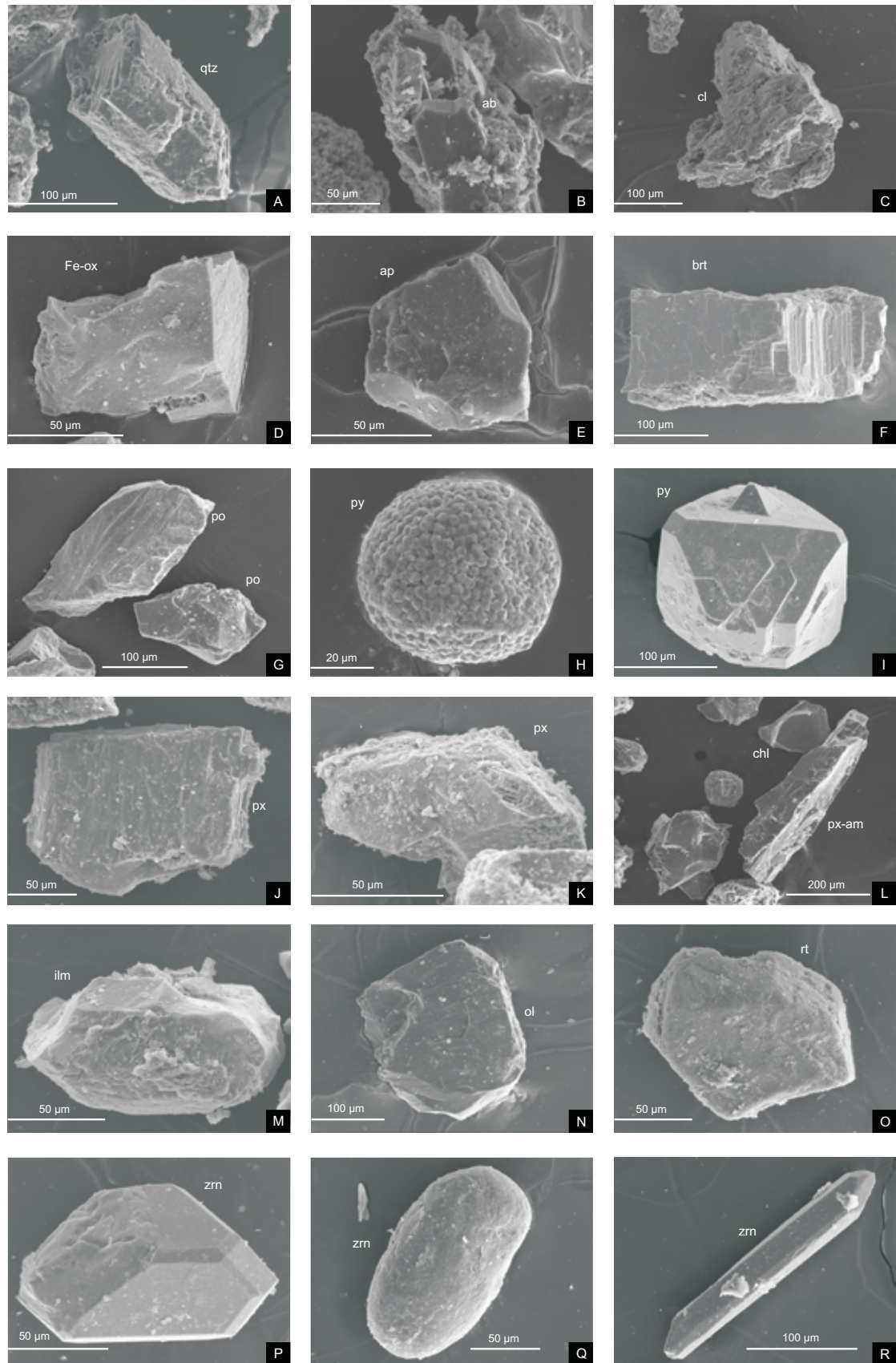


Figure 8. SEM images of mineral assemblages in insoluble residues. A – I: minerals of authigenic or possible detrital origin, J – R grains of pure detrital origin. A – quartz (69 m), B – albite (31.1 m), C – clay mineral (20.5 m), D – undetermined iron oxide – oxyhydroxide (20.5 m), E – apatite (9.7 m), F – barite (87.45 m), G – pyrrhotite (79.7 m), H – framboidal pyrite (69 m), I – bipyramidal pyrite (87.45 m), J – pyroxene – augite (112.7 m), K – pyroxene (9.7 m), L – grain of pyroxene/amphibole composition, chlorite and pyrite framboid (45.5 m), M – ilmenite (98.5 m), N – olivine (54.7 m), O – rutile (9.7 m), P – zircon (98.5 m), Q – zircon (65 m), R – zircon (79.7 m).

GRS – MS segment	m	qtz	dol	ank	or	micr	ab	plg	kln	mnt	gp	brt	ap	ms	mic	am	ep	px	ol	py	po	chpy	chl	glt	Fe – ox	rt	ilm	tit	zrn	crn		
G1	5	X				X														X	XXX		X		X							
G1	9.7	X			X	X			X									X au	X	XXX												
G2	13.9	X				X														X												
G2	16.2	X				X														XX												
G2	20.5	X				X														XX												
G3	31.1	X					XX													X												
G3	35	X		X					X											X sp					Xg							
G3	39.8	X																		X												
G3	42.6	X																		X												
G3	45.5	X												X						X												
G4	54.7	XX										X								X											XX	
G5	59.4	X																		X												
G5	60	X		X																X												
G5	61.7	X							X											X												
G5	65		X						X											XX	X										XXX	
G5	69																			X fr												
G5	72.2																			X												
G5	76.1	X																		X												
G6	78.55	X	XXX						X									Xen		X												
G6	79.7	XXX	XX						X		X									X bi	X										XXX	
G7	81.7	XX							X											X												
G7	84.5	X																		XX												
G7	87.45	X	X			X	X	X	X			XXX								X X?	X											X
G8	90.4	X							X											XX	X											
G8	91.95	XX							X											X												
G9	94	X																		X												
G9	96.7																			X												
G9	98.5	XX																		XX												XX
G9	101.55	X																		XX												
G9	105.7	X							X											X												
G9	108.25	X							X											X												
G9	110	X							X											X												
G10	112.7	X																		X												
G10	113.55	X		X																XX												
G10	118.0																			XXX												
G11	118.15	X																		XX sp												
G11	118.9	X																		XX												XXX

Table 3. List of minerals identified in insoluble residue and whole – rock samples (EDX, X-ray techniques analyses, SEM-EMP analyses of polished sections of heavy fraction and light fraction aggregates). List of minerals and abbreviations: qtz – quartz, dol – dolomite, ank – ankerite, or – orthoclase, micr – microcline, ab – albite, plg – plagioclase, kln – kaolinite, mnt – montmorillonite, gp – gypsum, brt – barite, ap – apatite, ms – muscovite, mic – undetermined mica, am – amphibole, ep – epidote, px – pyroxene, ol – olivine, py – pyrite, po – pyrrotite, chpy – chalcopyrite, chl – chlorite, glt – glauconite, Fe – ox – undetermined oxyhydroxides (hematite, magnetite, limonite; g – goethite), rt – rutile, ilm – ilmenite, tit – titanite, zrn – zircon, crn – corundum, question mark – uncertain measurement, bi – bipyramidal shape, sp – spherical shape, di – dipside, au – augite, en – enstatite, X – rare or single grain analysis (1–2 grains/analyzed sample), XX – several grains (3–5 grains/analyzed sample), XXX – very abundant (more than 5 grains/analyzed sample), G1 – G11 – GRS-MS segments.

G6, G7 and G9). The most unusual is the abundance of zircons in the “false” Koněprusy Limestone unit – in whitish and light-grey crinoidal calcarenites–calcirudites; see an image from a thin section in Plate 2 – D. Zircons have never been reported from unmetamorphosed limestones of such purity. Geochronological data on Archaean stromatolitic carbonates were revealed by Moorbath et al. (1987) or Jahn et al. (1990). Data on U-Pb SHRIMP dating of detrital zircons and C and O isotopic composition of Jiaobei marbles in China were reported by Tang et al. (2006) or data on the age of metamorphism of marbles in the Alps by Taylor & Kalsbeek (1990), Vavra et al. (1999) or Rubatto et al. (1999). A different habitus and fabrics of the zircons from the Požár 3 section suggest that several populations of different source and of different age can be distinguished (Fig. 8 – P, Q, R). The grain size varies from 30 up to 200 μm . Studies on these populations and studies on elemental and isotopic compositions are in progress.

4.3.1. Stratigraphic variations in mineralogy of non-carbonate particles and its relationship to MS-GRS logs

Major changes in the MS and GRS logs of section Požár 3 concentrate to the base of the Praha Fm. The distribution of minerals and their approximate relative proportions are given in Table 3. Generally, the Lochkov Fm. limestones differ from the overlying Praha Fm. limestones in a relatively higher abundance of pyrite–pyrrhotite assemblages and in lower abundance of iron oxides (mostly goethite than hematite). The presence of iron oxides (mostly hematite) is typical for rocks of the Praha Fm. where the occurrence together with lighter pinkish and red colour hues of limestone (e.g. Slivenec, Loděnice or pelagic Řeporyje Limestone rich in dacryoconarid fauna) is indicative of higher oxygenation of the oceanic water column and suggests the above mentioned (4.1.) slow rates of sedimentation. This is supported also by an elevated activity of microborers (e.g., Plate 2 – E, F) which has also geochemical indications (see 4.4.).

Pyrite morphology shows differences in the Lochkov, Zlíčov and Praha Fms. Euhedral grains are the most abundant and dominant crystal shapes occurring in all these formations, but pyrite in the Lochkov Fm. tends to be of rather spherical to framboidal shape (Fig. 8 – H), unlike that in the Praha Fm. with rather bipyramidal pyrite crystals (Fig. 8 – I). Spherical pyrite crystals were identified in the Lower Kotýs Limestone (39.8 m), framboid-like structure in the Upper Kotýs Limestone (69 m; Fig. 8 – H) and pyrite crystals of spherical shape in the Zlíčov Limestone. A huge number of studies on the framboid formation both in natural environments and laboratory conditions suggest microbial origin of the framboids as revealed by Folk (2005) or Gong et al. (2008). Other studies deal with grain-size distribution of framboids as an indicator of redox depositional settings (Wilkin et al., 1996) or processes leading to the framboid formation (Wilkin & Barnes, 1997 and further citation *ibidem*). With respect to the stratigraphical distribution of “dark” and suboxic Lochkov and Zlíčov Fm. limestone

lithotypes and “light” to “red” and oxic Praha Fm. limestone lithotypes, we can assume that the occurrence of these unusual pyrite shapes coincides with these levels and fits the interpretation of the environmental changes the in section Požár 3.

Pyrrhotite grains in the sediments (Roberts & Turner, 1993; van Velzen et al., 1993; Horng et al., 1998) can be of either detrital or authigenic origin. Despite the fact that it is considered to be mostly of authigenic origin (e.g. Roberts & Turner, 1993), Horng & Roberts (2006) proposed a detrital origin for pyrrhotite in Pliocene-Holocene sediments in Taiwan, and suggested metamorphic basement rocks as its source. They argued by very slow velocity of pyrrhotite formation below ~ 180 °C. Pyrrhotite formation in the limestones of the Lochkov Fm. may be rather of diagenetic origin as suggested by fluid inclusions and isotopic data on calcite veins in the Prague Synform: relevant studies suggest temperatures between 127 to 167 °C and depths around 1–4 km as a result of tectonic burial during the Variscan Orogeny (Halavínová et al., 2008).

The Lochkov Fm. differs from the overlying Praha Fm. also in a higher abundance of the grains of pyroxene/amphibole composition or olivine (with augite, diopside or enstatite characteristics) and rutile grains. This can be explained by a higher admixture of material of volcanic origin. In one polished section of heavy-fraction material (9.70 m; Průhon lithofacies), a grain of basalt-type rock was identified. Chemical compositions of diopside, ilmenite, microcline and plagioclase fit within the average composition of UCC-MCC (upper and middle continental crust) complexes and basaltic mounds (L. Ackerman – pers. comm.). Ilmenite itself is distributed both in the Lochkov and Praha formations.

Higher MS values in the Praha Fm. compared to those in the Lochkov Fm. and Zlíčov Fm. can be explained by higher abundances of iron oxides and particularly by the increased amounts of non-carbonate impurities delivered into depositional settings in the form of atmospheric dust. A decrease in the sedimentation rate is also indicated by the occurrence of elevated amounts of barite (barite identified in insoluble residues and in additional 10–30 kg whole-rock crushed samples) close above the base of the Praha Fm. (78.55 and 79.7 m) and stratigraphically higher (87.45 m). The position of the maximum detected barite enrichment in section Požár 3 (87.45 m) coincides with the maximum in the MS values (87–88 m; $71.53 \text{ m}^3/\text{kg} \times 10^{-9}$) and GRS-K and INAA-K concentrations (1.6 % and 1.47 % respectively) and correspond to the transgressive trend above the Lochkovian-Pragian boundary Event (Chlupáč & Kukul, 1988; Chlupáč et al., 1998).

4.4. Geochemical characteristics

4.4.1. REE

REE concentrations in all samples are listed in Table 4 and Fig. 9 – A, B, C.

The Praha Fm. is characterized by a steep gradient in LREE/HREE values and an increase in total REE concentrations. Mean value of the LREE/HREE ratio is

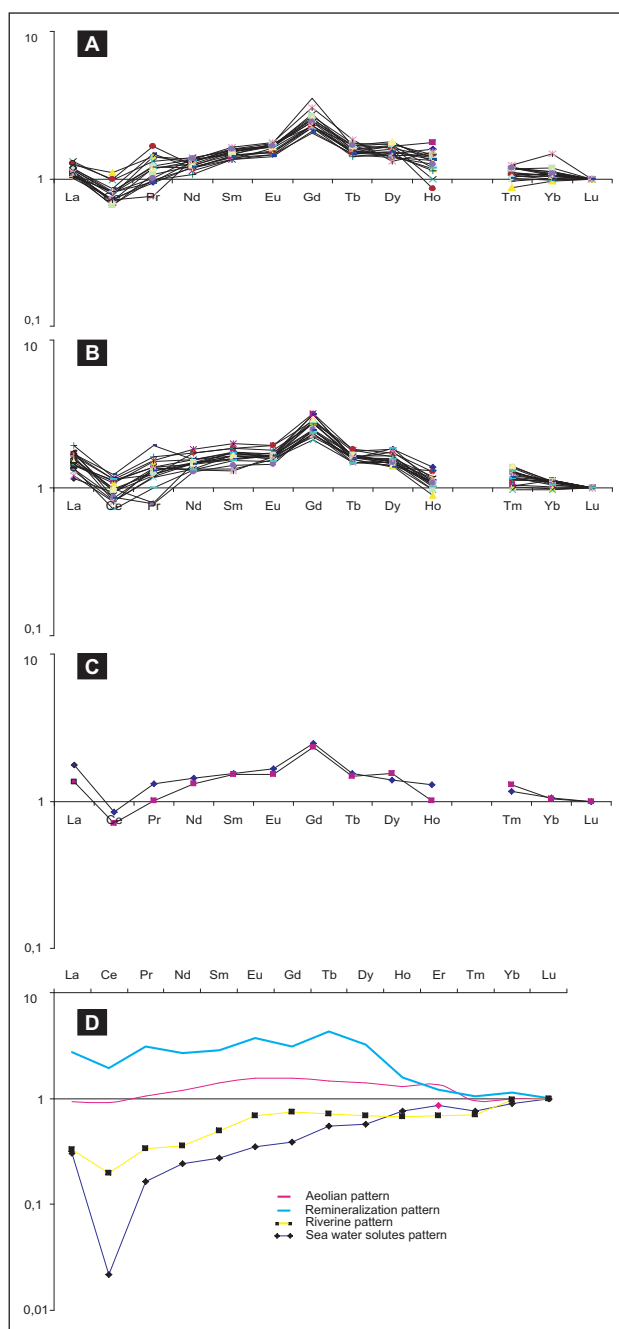


Figure 9. REE distributions for the Lochkov Fm. (A), Praha Fm. (B) and Zlíčov Fm. (C) showing patterns indication the aeolian source of impurities after Nozaki (2001). D – four ideal patterns: riverine, aeolian, sea water solutes and remineralization pattern). Note strong effects of remineralization (LREE down, e.g. Ce) and elevated HREE, MREE (e.g. Gd) owing to increased microbial activity in host rocks (mostly in the Praha Fm.).

0.92 for the Praha Fm. and 0.74 for the Lochkov and Zlíčov Fms. A decreasing trend in this ratio is visible through the entire Lochkov Fm. toward the base of the Praha Fm. and the same trend exists in the Praha Fm. toward the base of the Zlíčov Fm.

The PAAS and Lu-normalized distributions were used to identify the possible fluxes of non-carbonate impurities and were based on estimates made by Nozaki (2001). He revealed four general patterns: the aeolian (atmospheric),

riverine, sea water solutes and remineralization inputs of impurities into marine environment (Fig. 9 – D). The aeolian pattern is the most comparable to the REE distribution of PAAS, whereas the riverine pattern is slightly depleted in LREE (La to Sm). The sea water solutes pattern is highly depleted in LREE (mostly in Ce) than the previous, and the remineralization pattern is characterized by the enrichment in LREE. The REE distributions of the Lochkov, Praha and Zlíčov formations are most comparable to the aeolian type of impurities (Fig. 9 – A, B, C). If compared to the original pattern of Nozaki (2001) there could be a slight affection by the remineralization pattern (enrichment in LREE) and also sea water solutes pattern (strong Ce depletion, enrichment in HREE). Correlation coefficients are figured in Fig. 10.

A significant feature is the enrichment in Gd in all studied samples, most notably in the Praha Fm. and in samples from intervals with condensed sedimentation. Hirata et al. (2006), Takahashi et al. (2005; 2007) reported enrichment in HREE with the maximum in Sm and Eu due to the bacterial activity and similar patterns in bacteria-mediated iron oxides and oxyhydroxides such as banded-iron formations (BIF). Iron oxides of bacterial origin (hematite) in the Slivenec Limestone (Cikánka Quarry and outcrops near Srbsko; Mamet et al., 1997) and increased microborers activity in the “pink and red facies” of the Slivenec, Loděnice and Řeporyje Limestone members of the Praha Fm. in section Požár 3 suggest such an explanation of increased HREE concentrations. Mean values of Gd are 2.51 ppm for the Lochkov Fm., 2.95 ppm for the Slivenec Limestone, 2.83 ppm for the lighter parts of the Loděnice Limestone, and 2.69 ppm for the Řeporyje Limestone.

5. Discussion

5.1. Non-carbonate particles as an atmospheric supply

5.1.1. Pathway of detrital zircon delivery

The presence of detrital zircons and their morphology are strong indications that these particles were delivered into the marine environment mostly in the form of aeolian material. Prismatic type (e.g. Fig. 8 – R) occurs among clearly recycled grains (Fig. 8 – Q). These are rounded, with no crystal faces, possibly of very different ages or provenances. Their shape indicates an obvious re-sedimentation. On the other hand, the presence of prismatic zircon grains, very often non-fractured and unbroken (despite the length of 100–200 μm and the usual width of only 20–30 μm), with well-defined crystal faces suggests that they may not have been transported over long distances. They were transported as aeolian dust rather than with fluvial material where collisions of particles would have caused fracturing. Totally rounded grains could have been recycled by volcanic activity which produced prismatic types of these zircons, and they both could have been transported as volcanic material mixed with normal background material. As no volcanic ash in the form of bands or continuous intercalations was observed, either macroscopically nor microscopically, in limestone beds with zircon occurrence and no volcanic

m	La	Ce	Pr	Nd	Sm	Eu	Gd	Tb	Dy	Ho	Tm	Yb	Lu
5.0	0,227	0,159	0,188	0,261	0,309	0,332	0,500	0,304	0,293	0,317	0,232	0,221	0,198
9.7	0,207	0,138	0,189	0,226	0,271	0,290	0,426	0,294	0,320	0,337	0,210	0,201	0,192
13.9	0,269	0,238	0,303	0,290	0,320	0,358	0,528	0,323	0,311	0,252	0,188	0,209	0,216
16.2	0,262	0,195	0,261	0,278	0,309	0,334	0,551	0,312	0,332	0,198	0,212	0,200	0,200
20.5	0,230	0,141	n.d.	0,231	0,275	0,329	0,466	0,306	0,309	0,283	0,224	0,211	0,204
31.1	0,377	0,296	0,494	0,365	0,429	0,444	0,679	0,443	0,468	0,254	0,316	0,318	0,296
39.8	0,264	0,168	0,246	0,270	0,343	0,369	0,562	0,358	0,366	0,284	0,266	0,275	0,252
42.6	0,282	0,207	0,361	0,287	0,330	0,342	0,511	0,353	0,336	0,322	0,252	0,253	0,243
45.5	0,299	0,207	0,303	0,343	0,396	0,438	0,672	0,413	0,441	0,310	0,314	0,279	0,260
54.7	0,407	0,279	0,417	0,464	0,498	0,593	1,206	0,568	0,595	0,477	0,352	0,379	0,342
59.4	0,281	0,172	0,276	0,318	0,393	0,438	0,687	0,449	0,445	0,379	0,304	0,309	0,260
61.7	0,349	0,232	0,391	0,413	0,504	0,539	0,840	0,549	0,584	0,424	0,388	0,368	0,328
65.0	0,309	0,216	0,393	0,359	0,444	0,485	0,632	0,466	0,448	0,394	0,328	0,293	0,278
69.0	0,372	0,244	0,256	0,457	0,550	0,596	1,028	0,626	0,445	0,511	0,418	0,500	0,338
72.2	0,335	0,255	0,319	0,434	0,507	0,525	0,770	0,532	0,445	0,400	0,378	0,345	0,318
76.1	0,306	0,244	0,356	0,351	0,425	0,460	0,677	0,458	0,423	0,431	0,284	0,297	0,296
78.55	0,267	0,195	0,251	0,321	0,368	0,385	0,547	0,394	0,407	0,359	0,268	0,261	0,266
79.7	0,247	0,199	0,292	0,286	0,356	0,367	0,594	0,381	0,389	0,294	0,250	0,240	0,214
81.7	0,488	0,376	0,466	0,493	0,591	0,558	1,062	0,543	0,495	0,372	0,356	0,344	0,340
84.5	0,766	0,576	0,815	0,841	0,932	0,877	1,498	0,839	0,755	0,481	0,542	0,534	0,538
87.45	0,841	0,663	0,820	0,922	0,970	0,924	1,251	0,875	0,834	0,569	0,572	0,571	0,590
90.4	0,588	0,395	0,531	0,634	0,686	0,665	1,096	0,625	0,564	0,370	0,418	0,390	0,346
91.95	0,698	0,389	0,501	0,712	0,766	0,792	1,170	0,752	0,707	0,530	0,464	0,461	0,412
94.0	0,609	0,371	0,509	0,542	0,584	0,561	0,853	0,518	0,516	0,322	0,360	0,344	0,314
96.7	0,572	0,411	0,653	0,518	0,586	0,570	1,057	0,535	0,520	0,380	0,348	0,377	0,336
98.55	0,581	0,402	0,436	0,522	0,611	0,569	0,970	0,555	0,655	0,380	0,410	0,388	0,354
101.55	0,554	0,344	0,438	0,515	0,577	0,555	0,845	0,584	0,520	0,384	0,476	0,379	0,350
105.7	0,521	0,329	0,449	0,516	0,543	0,582	0,853	0,575	0,520	0,336	0,478	0,382	0,346
108.25	0,547	0,351	0,280	0,519	0,586	0,582	1,034	0,584	0,509	0,376	0,496	0,386	0,354
112.7	0,397	0,251	0,360	0,408	0,409	0,473	0,694	0,494	0,459	0,352	0,380	0,329	0,306
113.0	0,589	0,389	0,663	0,643	0,630	0,791	1,115	0,779	0,841	0,560	0,620	0,532	0,484
113.55	0,478	0,308	0,281	0,461	0,505	0,518	0,889	0,532	0,534	0,384	0,450	0,389	0,358
118.0	0,483	0,241	0,348	0,431	0,466	0,486	0,647	0,468	0,466	0,352	0,374	0,327	0,294
118.15	0,303	0,146	0,225	0,248	0,266	0,285	0,423	0,266	0,239	0,224	0,202	0,180	0,172
118.9	1,000	0,526	0,742	0,975	1,129	1,118	1,721	1,091	1,145	0,750	0,962	0,768	0,740

PAAS normalized

n.d. – not detected

Table 4. REE concentrations throughout the studied interval. Lochkov Fm. (0–77.5 m), Praha Fm. (77.6–118.1 m), Zlíchov Fm. (118.15–123.6 m).

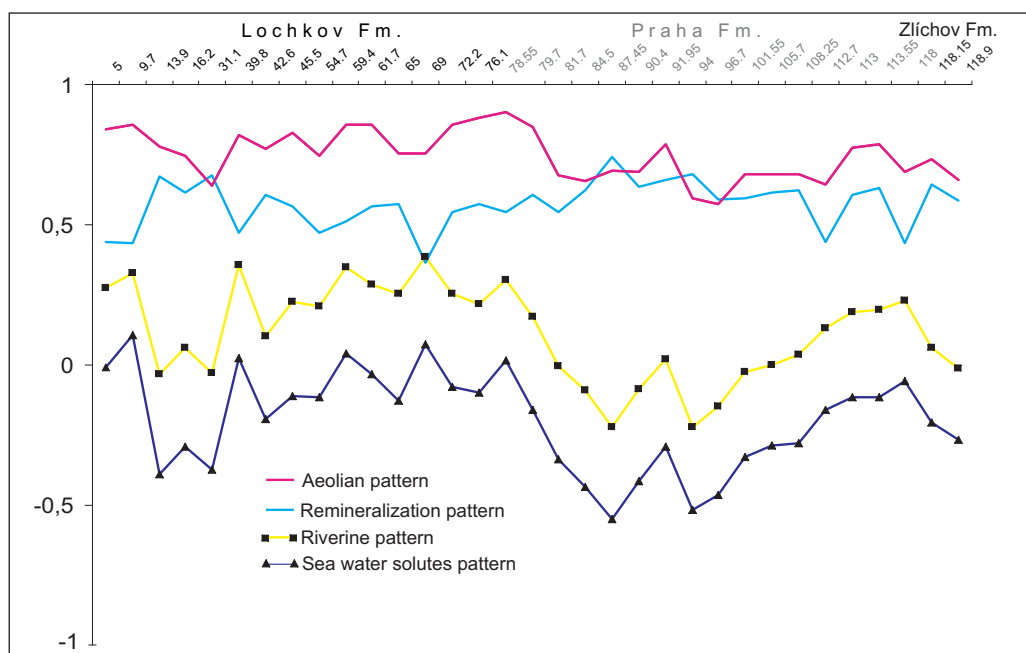


Figure 10. A correlation with four ideal REE patterns of different fluxes after Nozaki (2001).

activity is reported from the Prague Synform at this stratigraphic level, we can presume that these particles were transported in the form of atmospheric dust. Geochemical data on REE distributions point to the aeolian activity as the dominant process for the delivery of these detrital grains. Correlation coefficients of all samples from section Požár 3 plotted against ideal patterns after Nozaki (2001) are demonstrated in Fig. 10. The aeolian type of input shows a strong positive correlation (0.57 to 0.90) throughout the entire section, and this level is maintained (only with slight increase) up to the Zlíchov Fm. A decreasing trend in the correlation of fluvial source of impurities is clearly visible from the Lochkov Fm. (maximum 0.38) toward the Praha Fm. where it drops very quickly (to -0.22). In the upper parts of the Praha Fm., the correlation for the fluvial source increases again to slightly positive values (0.23) and vanishes again at the base of the Zlíchov Fm. (0 values). Indications of increased fluvial input in the zircon-bearing intervals do not correspond with the highest correlation coefficients for this pattern. A pattern typical for remineralization fully corresponds with lithology. It shows a stable, slightly positive correlation through the Lochkov Fm. and rapidly increases at the base of the Praha Fm., which fits the distribution of cement within the lithotypes. A stronger cementation is typical for the basal part of the Praha Fm. The sea water solutes pattern shows a slightly negative (Lochkov Fm., Zlíchov Fm.) to strongly negative correlation (Praha Fm.).

Unpublished very preliminary conclusions based on detrital zircons from the two levels (one in the Lochkovian and the second in the Pragian) and their age distributions suggest the broader spectra of ages and provenance displayed in the Pragian than in the Lochkovian which might suggest the change in the flux and the provenance of material delivered not by oceanic currents but as an atmospheric dust. It is in agreement with observations on

spores from the Lower and Middle Devonian limestones in the Prague Synform and their affinities revealed by several authors. Hladil & Bek (1998; 1999) reported plant spores assemblages of clear links to Ardenne/Rhenish/Moravian/Eastern Canada regions which is in contrast to the affinities of marine fauna. The Early/Middle Devonian marine benthic fauna of the Prague Synform has peri-Gondwanan characteristics together with Algeria, Morocco, France or Spain (Ibermaghian fauna) whereas spores have Laurussian affinity. Authors explain this different faunal and floral relation by the presence of land barriers between Laurussia and peri-Gondwanan area and the difference between ocean currents and wind directions and they propose a hypothetical southeasterly moving storms which might transport spores. Laurussian south margin might be much more close than the Gondwanan and they argued that Ibermaghian fauna of the Prague Synform and south Laurussian margin slightly differs whereas spore assemblages are very similar. Moreover Vavrdová (1989) reported miospores from the Lower Devonian Dvorce-Prokop Limestone from the neighbouring section Požár 2 and again with some of them of Ardenno-Rhenish affinities. It is still all in debate because relevant precise data on spore assemblages and their affinities from the lowermost Devonian or Silurian/Devonian boundary are missing as well as there is a lack of data on detrital zircon provenance which would permit us to put this change in this proposed interval.

5.1.2. Ba-K enriched level and possible climate change

Torres et al. (1996) and Bréhéret & Brumsack (2000) consider the presence of barite in pelagic environment far from hydrothermal activity an indicator of short-term breaks in sedimentation or reduced sedimentation rates: these allow the formation of a barite diagenetic front with precipitated barite nodules. Bishop (1988) and Riedinger et al. (2006 and further citations *ibidem*) postulated that

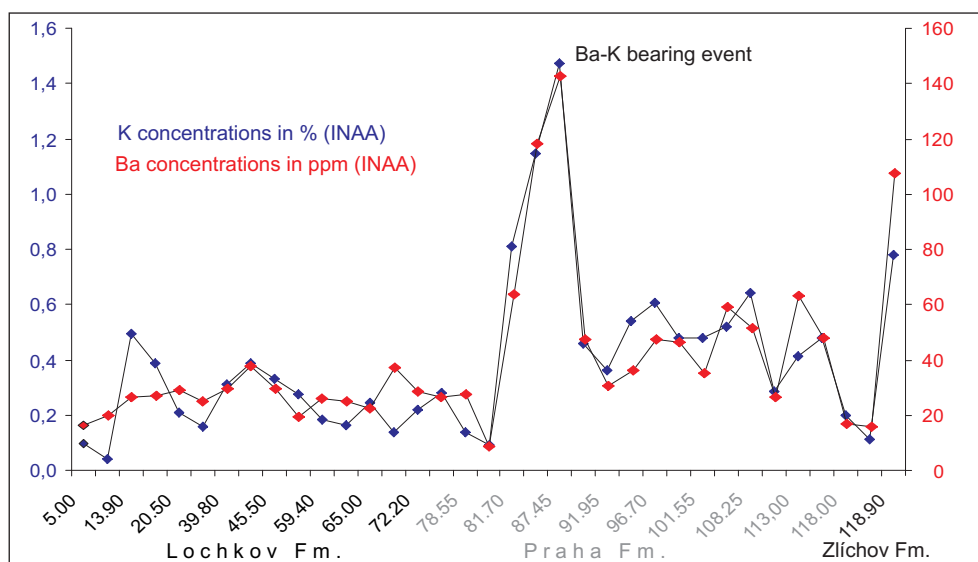


Figure 11. Variations in Ba and K (INAA) concentrations and position of Ba-K event.

Ba-enriched sediments very often underlie sediments with increased bioproductivity horizons and increased phytoplankton decay in the water column. Elevated concentrations of Ba and K (Fig. 11) within the interval 81.7 up to 87.45 m (medium-grey to dark grey Slivenec Limestone to Slivenec/Loděnice Limestone) may signify the presence of hydrothermal activity and host-rock alteration but the coincidence with elevated K concentrations can exclude this. This strong enhancement together with the maximum values of the MS might indicate a stronger flux of non-carbonate impurities connected with slow rates of sedimentation and decrease in carbonate productivity. This observation is supported by conodont biostratigraphy (Slavík et al., 2007) which may suggest a strongly condensed sedimentation in the upper part of the Lochkov Fm. but mostly in the basal part of the Praha Fm. and permit to conclude that this interval represents a change in the delivery of non-carbonate impurities during the possibly slower sedimentation, or reflects a major atmospheric change e.g. change in wind direction. Global climate change cannot be excluded because Lochkovian/Pragian sea-level fall is well documented worldwide e.g. from the Appalachian basin (Brett & Ver Straeten, 1997), eastern Australia (Talent & Yolkin, 1987), north Africa or Europe (Chlupáč & Kukul, 1988 and citations ibidem) and represent significant change from the Lochkovian strata. Hladil et al. (2008) propose that the Pragian was a period with extremely low sea level and “hot and humid” climate with intense chemical weathering on emerged lands which might be the source of increased delivery of impurities into oceans. It is in contrast to the Buggisch & Joachimski (2006) which interpret the oxygen isotopic data on the Pragian conodonts as a period with cooler climate than the Lochkovian. According to geochemical data (increased concentration of K, Th, enrichment in LREE, REE distribution), the presence of slightly different populations of detrital zircons and higher amounts of mineral phases of paramagnetic characteristics in the Pragian in the Požár 3 sections authors tend to agree with the first interpretation.

6. Conclusions

Such complex data on the MS and GRS logs, the combination with the analysis of stratigraphic variations in the composition of detrital grain assemblages of fine-grained non-carbonate impurities trapped in the limestones plotted against a lithological characteristics with geochemical data control are revealed for the first time. It turned out that these methods together with the study of insoluble residues provide a very reliable tool for the interpretation of variations in the delivery of non-carbonated impurities. Major changes concentrate to the proximity of the Lochkovian/Pragian boundary (~ Lochkov/Praha Fm.). The Praha Fm. provides a very stable pattern with elevated K and Th concentrations (Th/U ratio close to 4) whereas the underlying and overlying Lochkov Fm. and Zlíčov Fm. patterns are marked by low K concentrations and by the Th/U ratio below or around 1. This is interpreted as an increase in the flux of non-carbonate impurities mostly of paramagnetic characteristics. The proportions minerals which can carry MS properties in section Požár 3 (of ferromagnetic and paramagnetic characteristics), e.g., iron oxides, pyrrhotite, ilmenite, pyroxene, amphibole, olivine, chlorite, glauconite, clay minerals, ankerite, pyrite, chalcopyrite, epidote, vary along the section. To sum up, the Lochkov Fm. (and partly also the Zlíčov Fm.) is characterized by a higher abundance of the pyrite–pyrrhotite assemblage (related to the proportion of iron oxides, mostly goethite, which are also present but in low quantities) whereas the opposite is true for the Praha Fm. where iron oxides (mostly hematite) are abundant. Grains of ferromagnetic properties occur both in the Lochkov and Praha Fm. Due to the fact that the MS values are five times higher in the Praha Fm. than in the Lochkov and Zlíčov formations, we can assume that paramagnetic particles are rather responsible for the overall MS signal. This is strengthened by elevated K concentrations in the entire Praha Fm. with the maximum in the basal part (~ 81 to 87 m; both from INAA analyses and GRS data) and peak barite concentrations at the same level (as well as significantly

elevated Ba concentrations from INAA analyses). The occurrence of detrital zircon assemblages, which comprise also non-fractured and undamaged grains of prismatic type (up to 200 µm in diameter), is indicative of their aeolian origin rather than a fluvial source of input. Very preliminary and unpublished data on the ages of zircon populations from the Lochkovian and the Pragian shows different age displays and broader source material on the Pragian than the Lochkovian. REE distributions in whole-rock samples are also indicative of a flux of impurities into marine environment from an aeolian source according to the four general patterns introduced by Nozaki (2001). This REE distribution pattern is best comparable to PAAS distributions.

7. Acknowledgements

Funding for this project was supplied by the Grant Agency of the Czech Republic (project No. IAA300130702 and 210/10/2351) and the Research Plan of the Institute of Geology AS CR, v.v.i (AVOZ30130516). This study also contributes to IGCP Project No. 580. We also greatly appreciate an agreeable cooperation with Milan Trnka (Pikaso Ltd. – Řeporyje Quarry, crushed stone production). Vlasta Böhmová, Zuzana Korbelová and Anna Langrová (Laboratory of Physical Properties of Rocks, Institute of Geology AS CR, v.v.i.) are acknowledged for SEM-EMP analyses, Alžběta Svitáčková and Adrián Biroň (Geological Institute, Slovak Academy of Sciences) for TOC analyses, Jaroslav Frána (Institute of Nuclear Physics AS CR, v.v.i.) for INAA analyses. Authors gratefully thank to reviewers Johan Yans and Eberhard Schindler for improving this paper and valuable comments.

8. References

- AIGNER, T., SCHAUER, M., JUNGHANS, W.D. & REINHARD, T. L., 1995. Outcrop gamma-ray logging and its applications: examples from the German Triassic. *Sedimentary Geology*, 100: 47-61.
- ALLEN, J.R.M., BRANDT, U., BRAUER, A., HUBBERTEN, H.W., HUNTLEY, B., KELLER, J., KRAML, M., MACKENSEN, A., MINGRAM, J., NNEGENDANK, J.F.W., NOWACZYK, N.R., OBRHÄNSLI, H., WATTS, W.A., WULF, S. & ZOLITSCHKA, B., 1999. Rapid environmental changes in southern Europe during the last glacial period. *Nature*, 400: 740-743.
- BÁBEK, O., KALVODA, J., ARETZ, M., COSSEY, P.J., DEVUYST, F.X., HERBIG, H.G. & SEVASTOPULO, G., 2010. The correlation potential of magnetic susceptibility and outcrop gamma-ray logs at Tournaisian-Viséan boundary sections in Western Europe. *Geologica Belgica*, this volume.
- BÁBEK, O., PŘIKRYL, T. & HLADIL, J., 2007. Progressive drowning of carbonate platform in the Moravo-Silesian Basin (Czech Republic) before the Frasnian/Famennian event: facies, compositional variations and gamma-ray spectrometry. *Facies*, 53: 293-316.
- BISHOP, J.K.B., 1988. The barite-opal-organic carbon association in oceanic particulate matter. *Nature*, 331: 341-343.
- BRÉHÉRET, J.-G. & BRUMSACK, H.-J., 2000. Barite concretions as evidence of pauses in sedimentation in the Marnes Bleues Formation of the Vocontian Basin (SE France). *Sedimentary Geology*, 130: 205-228.
- BRETT, C.E. & VER STRAETEN, C.A., 1997. *Devonian Cyclicality and Sequence Stratigraphy in New York State. Field Trip Guidebook*. University of Rochester, Rochester.
- BUGGISCH, W. & JOACHIMSKI, M.M., 2006. Carbon isotope stratigraphy of the Devonian of Central and Southern Europe. *Palaeogeography, Palaeoclimatology, Palaeoecology*, 240: 68-88.
- CARLS, P., SLAVÍK, L. & VALENZUELA-RÍOS, J.I., 2007. Revisions of conodont biostratigraphy across the Silurian-Devonian boundary. *Bulletin of Geosciences*: 82, 145-164.
- CARLS, P., SLAVÍK, L. & VALENZUELA-RÍOS, J.I., 2008. Comments on the GSSP for the basal Emsian stage boundary: the need for its redefinition. *Bulletin of Geosciences*, 83: 383-390.
- CHÁB, J., BREITER, K., FATKA, O., HLADIL, J., KALVODA, J., ŠIMŮNEK, Z., ŠTORCH, P., VAŠÍČEK, Z., ZAJÍC, J. & ZAPLETAL, J., 2008. Stručná geologie základu Českého masivu a jeho karbonského a permského pokryvu. *Vydavatelství České geologické služby*, Praha. [In Czech].
- CHLUPÁČ, I., 1953. Stratigraphical investigation of the border strata of the Silurian and the Devonian in Central Bohemia. (English summary). *Sborník Ústředního ústavu geologického, Oddíl geologický*, 20: 277-347.
- CHLUPÁČ, I., 1981. Stratigraphic terminology of the Devonian in Central Bohemia (Barrandian area, Czechoslovakia). *Věstník Ústředního ústavu geologického*, 56: 263-270.
- CHLUPÁČ, I. & KUKAL, Z., 1988. Possible global events and the stratigraphy of the Palaeozoic of the Barrandian (Cambrian – Middle Devonian, Czechoslovakia). *Sborník geologických věd, Geologie*, 43: 83-146.
- CHLUPÁČ, I., HAVLÍČEK, V., KŘÍŽ, J., KUKAL, Z. & ŠTORCH, P., 1998. *Palaeozoic of the Barrandian*. Czech Geological Survey. Prague.
- CRICK, R.E., ELLWOOD, B.B., EL HASSANI, A. & FEIST, R., 2000. Proposed magnetostratigraphy susceptibility magnetostratotype for the Eifelian-Givetian GSSP (Anti-Atlas, Morocco). *Episodes*, 23: 93-101.
- CRICK, R.E., ELLWOOD, B.B., FEIST, R. & HLADIL, J., 1997a. Magnetostratigraphy event and cyclostratigraphy (MSEC) of the Eifelian-Givetian GSSP and associated boundary sequences in North Africa and Europe. *Episodes*, 20: 167-175.

- CRICK, R.E., ELLWOOD, B.B., EL HASSANI, A., FEIST, R. & HLADIL, J., 1997b. *Magnetostratigraphy event and cyclostratigraphy, MSEC - its use in characterizing the Eifelian-Givetian boundary sequence, the Kačák-otomari event, and in determining the duration of the Eifelian and Givetian*. The Amadeus Grabau Symposium, Abstracts. Rochester, New York: 23.
- CRICK, R.E., ELLWOOD, B.B., EL HASSANI, A., HLADIL, J., HROUDA, F. & CHLUPÁČ, I., 2001. Magnetostratigraphy (MSEC) of the Pridolian-Lochkovian GSSP (Klonk, Czech Republic) and coeval sequences in Anti-Atlas (Morocco). *Palaeogeography, Palaeoclimatology, Palaeoecology*, 167: 73-100.
- CRICK, R.E., ELLWOOD, B.B., FEIST, R., EL HASSANI, A., SCHINDLER, E., DREESEN, R., OVER, J. & GIRARD, C., 2002. Magnetostratigraphy susceptibility of the Frasnian/Famennian boundary. *Palaeogeography, Palaeoclimatology and Palaeoecology*, 181: 67-90.
- DA SILVA, A.C., POTMA, K., WEISSENBERGER, J.A.W., WHALEN, M., HUMBLET, M., MABILLE, C. & BOULVAIN, F., 2009. Magnetic susceptibility evolution and sedimentary environments on carbonate platform sediments and atolls, comparison of the Frasnian from Belgium and Alberta, Canada. *Sedimentary Geology*, 214: 3-18.
- ELLWOOD, B.B., CRICK, R.E., EL HASSANI, A., BENOIST, S.L. & YOUNG, R.H., 2000. Magnetostratigraphy method applied to marine rocks: Detrital input versus carbonate productivity. *Geology*, 28: 1135-1138.
- ELLWOOD, B.B., TOMKIN, J.H., RATCLIFFE, K.T., WRIGHT, M. & KAFIFY, A.M., 2008. High-resolution magnetic susceptibility and geochemistry for the Cenomanian/Turonian boundary GSSP with correlation to time equivalent core. *Palaeogeography, Palaeoclimatology and Palaeoecology*, 261: 105-126.
- ELLWOOD, B.B., CRICK, R.E., GARCÍA-ALCALDE FERNANDEZ, J.L., SOTO, F.M., TRUYÓLS-MASSONI, M., EL HASSANI, A. & KOVAS, E.J., 2001. Global correlation using magnetic susceptibility data from Lower Devonian rocks. *Geology*, 29: 583-586.
- FIET, N. & GORIN, G.E., 2000. Gamma-ray spectrometry as a tool for stratigraphic correlations in the carbonate-dominated, organic-rich, pelagic Albian sediments in Central Italy. *Eclogae Geologicae Helvetiae*, 93: 175-181.
- FLÜGEL, E., 2004. *Microfacies of Carbonate Rocks. Analysis, Interpretation and Application*. Springer-Verlag, Berlin, Heidelberg, New York.
- FOLK, J.L., 2005. Nannobacteria and the formation of framboidal pyrite: Textural evidence. *Journal of Earth System Science*, 114: 369-374.
- FU, S., 1991. Funktion, Verhalten und Einteilung fucoider und lophoctenoider Lebensspuren. *Courier Forschungsinstitut Senckenberg*, 35: 1-79. [In German].
- GLASMACHER, U., MANN, U. & WAGNER, G. A., 2002. Thermotectonic evolution of the Barrandian, Czech Republic as revealed by apatite fission-track analysis. *Tectonophysics*, 359: 381-402.
- GONG, Y.-M., SHI, G.R., WELDON, E.A., DU, Y.-S. & XU, R., 2008. Pyrite framboids interpreted as microbial colonies within the Permian *Zoophycos* spreiten from southeastern Australia. *Geological Magazine*, 145: 95-103.
- HALAVÍNOVÁ, M., MELICHAR, R. & SLOBODNÍK, M., 2008. Hydrothermal veins linked with the Variscan structure of the Prague Synform (Barrandien, Czech Republic): resolving fluid-wall rock interaction. *Geological Quarterly*, 52: 309-320.
- HAVLÍČEK, V., 1981. Development of a linear sedimentary depression exemplified by the Prague basin (Ordovician - Middle Devonian; Barrandian area - central Bohemia). *Sborník geologických věd, Geologie*, 35: 7-48.
- HAVLÍČEK, V., 1982. Ordovician in the Bohemia: Development of the Prague Basin and its benthic communities. *Sborník geologických věd, Geologie*, 37: 103-136.
- HELLER, F. & EVANS, M.E., 1995. Loess magnetism. *Revue of Geophysics*, 33: 211-240.
- HIRATA, T., TAKAHASHI, Y. & FORTIN, D., 2006. Evidence from REE patterns for microbial contribution to the formation of natural Fe oxides and BIF. *Geochimica et Cosmochimica Acta*, 70, Supplement 1: A253.
- HLADIL, J., 2002. Geophysical records of dispersed weathering products on the Frasnian carbonate platform and early famennian ramps in Moravia, Czech Republic: proxies for eustasy and paleoclimate. *Palaeogeography, Palaeoclimatology, Palaeoecology*, 181: 213-250.
- HLADIL, J. & BEK, J., 1998. Dispersal of marine fauna and spores of continental plants: Implication for hydrospheric/atmospheric circulation pattern and paleogeography (Devonian, Emsian-Eifelian, NGM/SLM). *Schriften des Staatlichen Museums für Mineralogie und Geologie zu Dresden*, 9: 147-148.
- HLADIL, J. & BEK, J., 1999. Distances between the Early/Middle Devonian Gondwana and Laurussia; faunal and spore dispersals as compared with paleomagnetic data on paleolatitudes. *Exploration Geophysics, Remote Sensing and Environment*, 5 (1998): 29-33.
- HLADIL, J. & KALVODA, J., 1997. A short range anomaly in the earliest Emsian sedimentation of the Barrandian: possible reflection of widely controlled or global event. *Subcommission on the Devonian Stratigraphy, Newsletter*, 13: 37-38.
- HLADIL, J. & PRUNER, P., 2001. Anatomy of the Kacák-related magnetostratigraphic zones (Devonian) based on the carbonate deposits at medium rate of sedimentation. *Geophysical Research Abstracts, EGS26 Nice - Katlenburg-Lindau*, 3: 1203.

- HLADIL, J., CEJCHAN, P., BABEK, O., KOPTIKOVA, L., NAVRATIL, T. & KUBINOVA, P., 2010. Dust – A geology-orientated attempt to reappraise the natural components, amounts, inputs to sediment, and importance for correlation purposes. *Geologica Belgica*, this volume.
- HLADIL, J., ČEJCHAN, P., GABAŠOVÁ, A., TÁBORSKÝ, Z. & HLADÍKOVÁ, J., 1996. Sedimentology and orientation of tentaculite shells in turbidite lime mudstone to packstone: Lower Devonian, Barrandian, Bohemia. *Journal of Sedimentary Research*, 66: 888-899.
- HLADIL, J., GERSL, M., STRNAD, L., FRANA, J., LANGROVA, A. & SPISIAK, J., 2006. Stratigraphic variations of complex impurities in platform limestones and possible significance of atmospheric dust: a study with emphasis on gamma-ray spectrometry and magnetic susceptibility outcrop logging (Eifelian-Frasnian, Moravia, Czech Republic). *International Journal of Earth Sciences (Geologische Rundschau)*, 95: 703-723.
- HLADIL, J., SLAVÍK, L., SCHNABL, P., KOPTÍKOVÁ, L., FRÁNA, J., VACEK, F. & BÁBEK, O., 2008. The gross environmental phenomenon of the classical Pragian stage (“hot lowstand”). In X-CD Technologies, Bjorlykke, A. (ed.), 33rd International Geological Congress, International Union of Geological Sciences. Abstract CD-ROM, HPF-01 General contributions to paleontology and historical geology, Part 1, Oslo: 1343454.
- HLADIL, J., BOSAK, P., JANSKA L.F., TEZKY, A., HELESICOVA, K., HRUBANOVA, J., PRUNER, P., KRUTA, M., SPACEK, P. & CHADIMA, M., 2000. Frasnian eustatic cycles viewed with gamma spectrometric and magnetosusceptibility stratigraphy tools, Moravia - six major floodings on cratonized basement. *Subcommission on Devonian Stratigraphy Newsletter*, 17: 48-52.
- HLADIL, J., KOPTÍKOVÁ, L., GALLE, A., SEDLÁČEK, V., PRUNER, P., SCHNABL, P., LANGROVÁ, A., BÁBEK, O., FRÁNA, J., HLADÍKOVÁ, J., OTAVA, J. & GERŠL, M., 2009. Early Middle Frasnian platform reef strata in the Moravian Karst interpreted as recording the atmospheric dust changes: the key to understanding perturbations in the *punctata* conodont Zone. *Bulletin of Geosciences*, 84: 75-106.
- HORNG, C.S. & ROBERTS, A.P., 2006. Authigenic or detrital origin of pyrrhotite in sediments? Resolving a paleomagnetic conundrum. *Earth and Planetary Science Letters*, 241: 750-762.
- HORNG, C.S., TORII, M., SHEA, K.S. & KAO, S.J., 1998. Inconsistent magnetic polarities between greigite- and pyrrhotite/magnetite-bearing marine sediments from the Tsailiao-chi section, southwestern Taiwan. *Earth and Planetary Science Letters*, 164: 467-481.
- JAHN, B.-M., BERTRAND-SARFATI, J., MORIN, N. & MACE, J., 1990. Direct dating of stromatolitic carbonates from the Schmidtsdrif Formation (Transvaal Dolomite), South Africa, with implications on the age of the Ventersdorp Supergroup. *Geology*, 18: 1211-1214.
- JOHNSON, J.G. & MURPHY, M.A., 1984. Time-rock model for Siluro-Devonian continental shelf, western United States. *Bulletin of the Geological Society of America*, 95: 1349-1359.
- JOHNSON, J. G., KLAPPER, G. & SANDBERG, G. A., 1985. Devonian eustatic fluctuations in Euramerica. *Bulletin of the Geological Society of America*, 96: 567-587.
- KOPTÍKOVÁ, L., BÁBEK, O., HLADIL, J., KALVODA, J. & SLAVÍK, L., 2010. Stratigraphic significance and resolution of spectral reflectance logs in Lower Devonian carbonates of the Barrandian area, Czech Republic; a correlation with magnetic susceptibility and gamma-ray logs. *Sedimentary Geology*, 225: 83-98.
- KOREN, T.N., KIM, A.I. & WALLISER, O.H., 2007. Contribution to the biostratigraphy around the Lochkovian-Pragian boundary in Central Asia (graptolites, tentaculites, conodonts). *Palaeobiodiversity and Palaeoenvironments*, 87: 187-219.
- LOWDER, W.M., CONDON, W.J. & BECK, H.I., 1964. Field spectrometric investigations of environmental radiation in the U.S.A. In Adams, J.A.S. & Lowder, W. (eds), *The Natural Radiation Environment*. University of Chicago Press, Chicago, 597-616.
- MACHADO, G., HLADIL, J., SLAVÍK, L., KOPTÍKOVÁ, L., MOREIRA, N., FONSECA, M. & FONSECA, P., 2010. An Emsian-Eifelian Calciturbidite sequence and the possible correlatable pattern of the Basal Choteč event in Western Ossa-Morena Zone, Portugal (Odivelas Limestone). *Geologica Belgica*, this volume.
- MAMET, B., PRÉAT, A. & DERIDDER, C., 1997. Bacterial Origin of the Red Pigmentation in the Devonian Slivenec Limestone, Czech Republic. *Facies*: 36, 173-188.
- MELICHAR, R., 2004. Tectonics of the Prague Synform: a hundred years of scientific discussion. *Krystalinikum*, 30: 167-187.
- MICHEL, J., BOULVAIN, F., PHILIPPO, S. & DA SILVA, A.C., 2010. Himmelbaach quarry (Mid Emsian, Luxemburg): palaeoenvironmental study and small scale correlations by facies and magnetic susceptibility. *Geologica Belgica*, this volume.
- MOORBATH, S., TAYLOR, P.N., ORPEN, J.L., TRELOAR, P. & WILSON, J.F., 1987. First direct radiometric dating of Archaean stromatolite limestone. *Nature*, 326: 865-867.
- NOZAKI, Y., 2001. Rare earth elements and their isotopes. In Steele, J.S., Turekian, K.K. & Thorpe, S.A. (eds), *Encyclopedia of Ocean Sciences*. Academic, London, 2354-2366.
- RADDADI, M.C., VANNEAU, A.A., POUPEAU, G., CARRIO-SCHAFFHAUSER, E., ARNAUD, H. & RIVERA, A., 2005. Interpretation of gamma-ray logs: The distribution of uranium in carbonate platform. *Comptes Rendus Geosciences*, 337: 1457-1461.

- ŘANDA, Z. & KREISINGER, F., 1983. Tables of nuclear constants for gamma-activation analysis. *Journal of Radioanalytical Chemistry*, 77: 279-495.
- ŘANDA, Z., FRÁNA, J., MIZERA, J., KUČERA, J., NOVÁK, J.K., ULRYCH, J., BELOV, A.G. & MASLOV, O.D., 2007. Instrumental neutron and photon activation analysis in the geochemical study of phonolitic and trachytic rocks. *Geostandards and Geoanalytical Research*, 31: 275-283.
- RIDER, M.H., 1986. *The Geological Interpretation of Well Logs*. Blackie and Son Limited, Glasgow.
- RIEDINGER, N., KASTEN, A., GRÖGER, J., FRANKE, C. & PFEIFER, K., 2006. Active and buried authigenic barite fronts in sediments from the Eastern Cape Basin. *Earth and Planetary Science Letters*, 886: 876-887.
- RIQUIER, L., AVERBUCH, O., TRIBOVILLARD, N., ALBANI, A.E., LAZREQ, N. & CHAKIRI, S., 2007. Environmental changes at the Frasnian–Famennian boundary in Central Morocco (Northern Gondwana): integrated rock-magnetic and geochemical studies. In Becker, R.T. & Kirchgasser, W.T. (eds), *Devonian Events and Correlation*. *Geological Society, London, Special Publications*, 278: 197-217.
- ROBERTS, A.P. & TURNER, G.M., 1993. Diagenetic formation of ferrimagnetic iron sulphide minerals in rapidly deposited marine sediments, South Island, New Zealand. *Earth and Planetary Science Letters*, 115: 257-273.
- RUBATTO, D., GEBAUER, G. & COMPAGNONI, R., 1999. Dating of eclogitefacies zircons: the age of Alpine metamorphism in the Sesia-Lanzo Zone (Western Alps). *Earth and Planetary Science Letters*, 167: 141-158.
- RUFFELL, A. & WORDEN, R., 2000. Palaeoclimate analysis using spectral gamma-ray data from the Aptian (Cretaceous) of southern England and southern France. *Palaeogeography, Palaeoclimatology, Palaeoecology*, 155: 265-283.
- SCHNABL, P., PRUNER, P., VENHODOVA, D., SLECHTA, S., KOPTIKOVA, L., VACEK, F. & HLADIL, J., 2009. State of the art in paleomagnetism of the Devonian limestones of the Prague Synform (Bohemium, Bohemian Massif). In Sobien, K. & Grabowski, J. (eds), *Paleomagnetic studies of Devonian rocks in Poland and Czech Republic: geological application*. Abstract Book. Polish Geological Institute, Warsaw, 28-31.
- SCHNEIDER, J., DE WALL, H., KONTNY, A. & BECHSTÄDT, T., 2004. Magnetic susceptibility variations in carbonates of the La Vid Group (Cantabrian Zone, NW-Spain) related to burial diagenesis. *Sedimentary Geology*, 166: 73-88.
- SLAVÍK, L., 2004a. The Pragian-Emsian conodont successions of the Barrandian area: search of an alternative to the GSSP polygnathid-based correlation concept. *Geobios*, 37: 454-470.
- SLAVÍK, L., 2004b. A new conodont zonation of the Pragian in the stratotype area (Barrandian, central Bohemia). *Newsletter on Stratigraphy*, 40: 39-71.
- SLAVÍK, L. & HLADIL, J., 2004. Lochkovian/Pragian GSSP revisited: evidence about conodont taxa and their stratigraphic distribution. *Newsletter on Stratigraphy*, 40: 137-153.
- SLAVÍK, L., VALENZUELA-RÍOS, J.I., HLADIL, J. & CARLS, P., 2007. Early Pragian conodont-based correlations between the Barrandian area and the Spanish Central Pyrenees. *Geological Journal*, 42: 499-512.
- TAKAHASHI, Y., CHATELLIER, X., HATTORI, K.H., KATO, K. & FORTIN, D., 2005. Adsorption of rare earth elements onto bacterial cell walls and its implication for REE sorption onto natural microbial mats. *Chemical Geology*, 219: 53-67.
- TAKAHASHI, Y., HIRATA, T., SHIMIZU, H., OZAKI, T. & FORTIN, D., 2007. A rare earth element signature of bacteria in natural waters? *Chemical Geology*, 244: 569-583.
- TALENT, J.A. & YOLKIN, E.A., 1987. Transgression-regression patterns for the Devonian of Australia and southern West Siberia. *Courier Forschungsinstitut Senckenberg*, 92: 235-249.
- TANG, J., ZHENG, Y.-F., WU, Y.-B. & GONG, B., 2006. Zircon SHRIMP U–Pb dating, C and O isotopes for impure marbles from the Jiaobei terrane in the Sulu orogen: Implication for tectonic affinity. *Precambrian Research*, 144: 1-18.
- TAYLOR, P.N. & KALSBECK, F., 1990. Dating of metamorphism of Precambrian marbles: examples from Proterozoic mobile belts in Greenland. *Chemical Geology*, 86: 21-28.
- TORRES, M.E., BRUMSACK, H.J., BOHRMANN, G. & EMEIS, K.C., 1996. Barite fronts in continental margin sediments: A new look at barium remobilization in the zone of sulfate reduction and formation of heavy barites in diagenetic fronts. *Chemical Geology*, 127: 125-139.
- UCHMAN, A., 1998. Taxonomy and ethology of flysch trace fossils: Revision of the Marian Książkiewicz collection and studies of complementary material. *Annales Societatis Geologorum Poloniae*, 68: 105-218.
- VACEK, F., 2007. Carbonate microfacies and depositional environments of the Silurian-Devonian boundary strata in the Barrandian area (Czech Republic). *Geologica Carpathica*, 58: 497-510.
- VAVRA, G., SCHMID, R. & GEBAUER, D., 1999. Internal morphology, habit and U–Th–Pb microanalysis of amphibolite to granulite facies zircon: geochronology of the Ivren Zone (Southern Alps). *Contributions to Mineralogy and Petrology*, 134: 380-404.
- VAVRDOVÁ, M., 1989. Early Devonian palynomorphs from the Dvorce-Prokop Limestone (Barrandian region, Czechoslovakia). *Věstník Ústředního ústavu geologického*, 64: 207-219.
- VAN VELZEN, A.J., DEKKERS, M.J. & ZIJDERVELD, J.D.A., 1993. Magnetic iron–nickel sulphides in the Pliocene and Pleistocene marine marls from the Vrica section (Calabria, Italy). *Earth and Planetary Science Letters*, 115: 43-55.

WALLISER, O.H., 1996. Global events in the Devonian and Carboniferous. *In* Walliser, O.H. (ed.), *Global events and event stratigraphy in the Phanerozoic*. Springer Verlag, Berlin, Heidelberg, New York, 225-250.

WENTWORTH, C.K., 1922. A scale of grade and class terms for clastic sediments. *Journal of Geology*, 30: 377-392.

WILKIN, R. T. & BARNES, H. L., 1997. Formation processes of framboidal pyrite. *Geochimica et Cosmochimica Acta*, 61: 323-39.

WILKIN, R.T., BARNES, H.L. & BRANTLEY, S.L., 1996. The size distribution of framboidal pyrite in modern sediments: An indicator of redox conditions. *Geochimica et Cosmochimica Acta*, 60: 3897-3912.

YOLKIN, E.A., KIM, A.I., WEDDIGE, K., TALENT, J.A. & HOUSE, M.R., 1997. Definition of the Pragian/Emsian Stage boundary. *Episodes*, 20: 235-240.

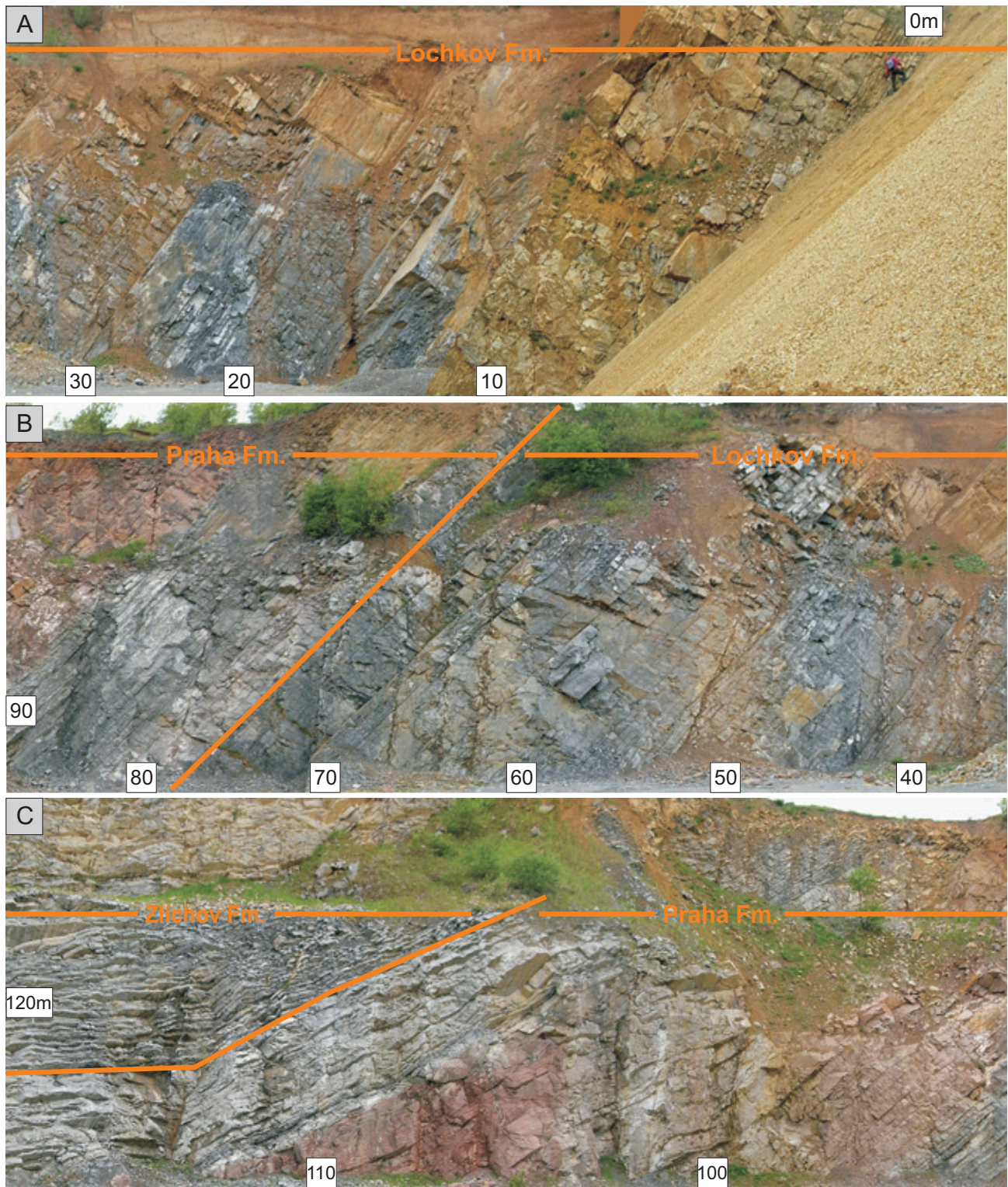


Plate 1. A panoramic picture of the Požár 3 section (divided into A, B, C parts). Numbers in white boxes are metres.

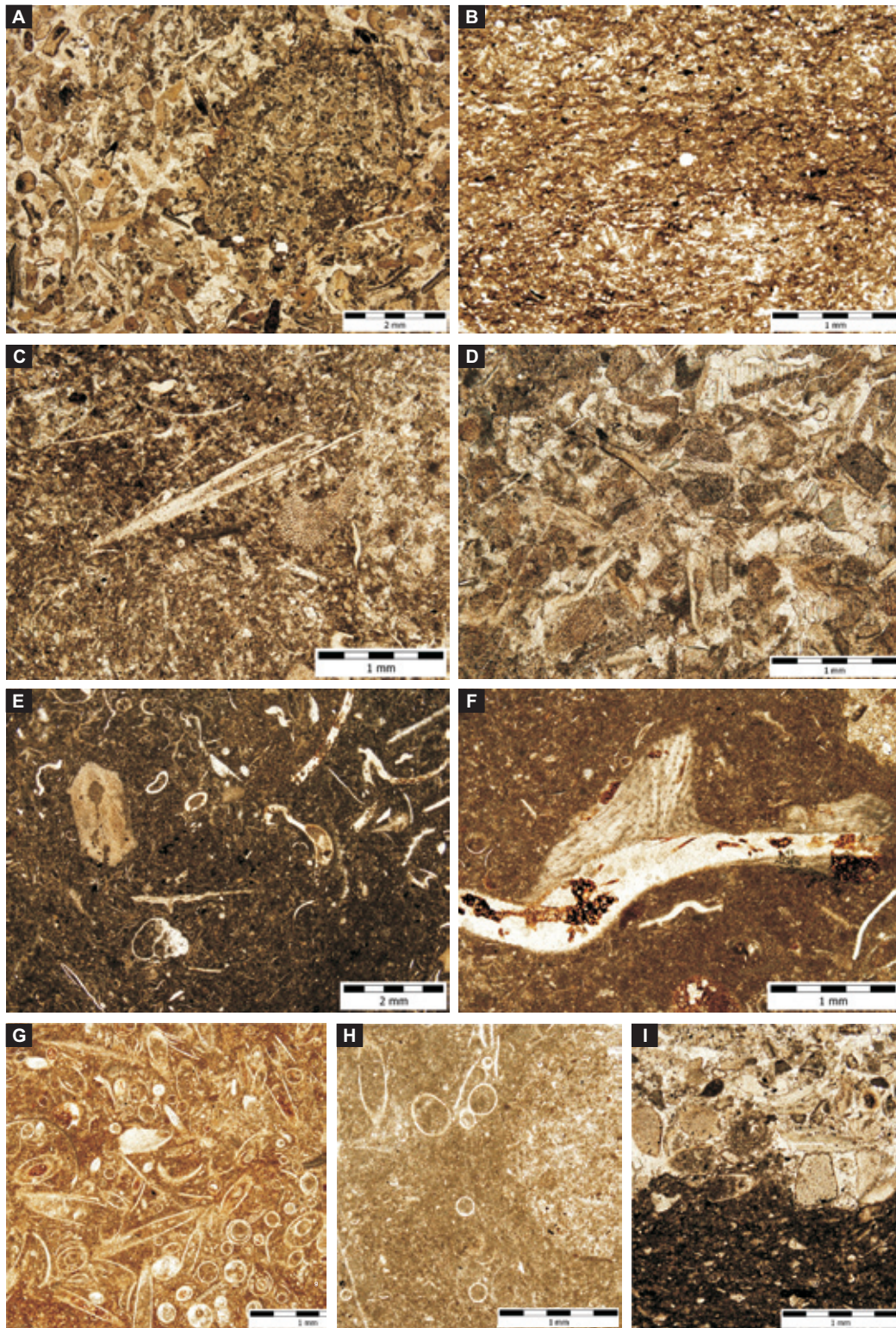


Plate 2. Thin section images from the main lithotypes from the Požár 3. A – C – Lochkov Fm., C – H – Praha Fm., I – Zlíchov Fm. A – Průhon lithotype (7 m) – crinoidal grainstone with micritized and coated grains, peloids, echinoderm and bryozoan fragments and peloidal grainstone intraclast, B – Radotín Limestone (16.5 m) – laminated spiculite, C – Upper Kotýs Limestone (74 m) – grainstone with crinoid, ostracod, brachiopod and trilobite fragments, slightly dolomitized, D – “false” Koněprusy Limestone (79.7 m) – crinoid – ostracod grainstone, note unimodal to bimodal grains size distribution; a zircon bearing bed, E – Slivenec Limestone (82 m) – calcisiltite with abundant bored trilobite and crinoid fragments, dactyloconarid and brachiopod shells with gastropods, note cement proportion decrease and strong multimodal grain-size distribution, F – Loděnice Limestone (100 m) – deeply bored trilobite fragment with affixed brachiopod, in the deeply burrowed calcisiltitic matrix dactyloconarid and ostracod shells prevail, G – Řeporyje Limestone (108 m) – dactyloconarid redbeds (calcisiltite/carbonated mud), note multiple insertions of dactyloconarid shells, H – Dvorce-Prokop Limestone (113.4 m) – the fifth bed of the “Graptolite event horizon” – burrowed calcisiltite with dactyloconarids, sponge spicules and crinoid fragments, I – Zlíchov Limestone (124 m) – dactyloconarid calcisiltite to carbonated mud (black shale intercalation) in the lower part of the thin section and crinoidal grainstone with brachiopod in the upper part.